CHALMERS
UNIVERSITY OF TECHNOLOGY

# Development and Implementation of test cells to perform DC and LI breakdown testing of materials used in HVDC cable accessories

Master's thesis in ELECTRIC POWER ENGINEERING

NEHRU SELVAN SELVASEKAR

DEPARTMENT OF ELECTRICAL ENGINEERING

CHALMERS UNIVERSITY OF TECHNOLOGY
Gothenburg, Sweden 2025
www.chalmers.se

Master's thesis 2025

# Development and Implementation of test cells to perform DC and LI breakdown testing of materials used in HVDC cable accessories

NEHRU SELVAN SELVASEKAR


CHALMERS
UNIVERSITY OF TECHNOLOGY

Department of Electrical Engineering
*Division of Electric Power Engineering*
Chalmers University of Technology
Gothenburg, Sweden 2025

Development and Implementation of test cells to perform DC and LI breakdown testing of materials used in HVDC cable accessories

NEHRU SELVAN SELVASEKAR



Supervisor (NKT): Sussane Nilsson, Head of R&D, Technology Basics - HV Cable Accessories Technology at NKT Accessories, Alingsås
Sajad Jafari, HV Specialist, Accessories Technology at NKT Accessories, Alingsås
Rashid Hussain, Senior HV Specialist, HV Accessories at NKT Accessories, Alingsås

Examiner (Chalmers): Yuriy Serdyuk, Professor, Department of Electrical Engineering, Division of Electric Power Engineering, Chalmers University of Technology

Master's Thesis 2025
Department of Electrical Engineering
Division of Electric Power Engineering
Chalmers University of Technology
SE-412 96 Gothenburg
Telephone +46 31 772 1000

Gothenburg, Sweden 2025

Development and Implemenatation of test cells to perform DC an LI breakdown testing of materials used in HVDC cable accessories

NEHRU SELVAN SELVASEKAR
Department of ELECTRICAL ENGINEERING
Chalmers University of Technology

# Abstract

The thesis work is to develop,build up and verify a test circuit for measurements of DC breakdown strength and LI testing.

The work contains both practical and theoretical elements, focusing on optimizing the design of electrodes as well as the size and shape of samples and to determine the Optimal dielectric properties of the insulation test medium using COMSOL Multiphysics. The aim of the work is to develop methods and design test setups for measuring both DC breakdown strength and Lightning Impulse testing, as a function of electric fields.

EPDM insulation and FGM are used in cable accessories considering EPDM rubber has low dielectric loss, making it ideal for high-voltage applications. FGM rubber can be produced by incorporating specific fillers and is designed to control and distribute electric fields within electrical insulation systems. Its main purpose is to prevent high electric field concentration, which can cause insulation breakdown and device failure.Rubber material is being tested using mechanical, chemical, and electrical methods. The dielectric test is one of the electrical testing methods used to determine the dielectric strength of rubber materials. Short-time and long-time tests are being carried out for dielectric testing. AC breakdown testing, DC breakdown testing, and LI breakdown testing on insulation EPDM and FGM samples are conducted using two different insulating liquids with variable permittivities to avoid surface flashover during a short test under international standards.

Designing a test cell for a dielectric test with an applied voltage of up to 150kV. Design the test cell (CAD model) and choose the electric field simulation with COMSOL Multiphysics software. To enhance development, the molded electrode test setup has been designed to eliminate the influence of the surrounding medium and facilitate future endurance testing.

Keywords: NKT, Cable accessories, AC breakdown testing, DC breakdown testing, LI breakdown testing, Mineral oil, Silicone oil, EPDM, FGM, COMSOL Multiphysics.

# Acknowledgements

This dissertation is based on both experimental and theoretical work conducted at NKT Accessories in Alingsås, Sweden. The research was carried out under the supervision of Yuriy Serdyuk, a professor in the Department of Electrical Engineering at Chalmers University of Technology, who provided invaluable technical support throughout my work.

I would like to express my sincere gratitude to my supervisor, Susanne Nilsson, Head of R&D Technology and Basics, Accessories Technology at NKT, for her helpful suggestions and for providing the testing equipment necessary for all the experiments in this study.

I am deeply thankful to my one of my supervisor, Sajjad Jafari, HV Specialist in Accessories Technology at NKT, who supported me from the beginning to the end of this project. His productive advice and continuous involvement have greatly contributed to my work. I would also like to special thank to another supervisor Rashid Hussain, Senior Specialist in HV Accessories at NKT, for his insightful advice and thorough review of this thesis, particularly regarding technical aspects and computer simulations. His guidance has significantly improved my writing skills.

I would like express my sincere gratitude to Jenny Hedlund, Klara-Lisa Jansson, Josefin Lundbjork, and Malte Hjartberg from the Chemical Laboratory, as well as Jerker Svensson and Christian Carlsson from the HV Laboratory, and Ekram Eljeiz, Georgios Batis, Ashish Jacob from the Design Team. I appreciate all their support. Additionally, I am grateful to my colleagues for creating a comfortable environment that allowed me to complete my work.

Last but not least, I want to express my heartfelt gratitude and respect to my wife, my parents, my grandparents, and my friends in India for their continuous love and unwavering support during my studies far from my home country.

Nehru selvan Selvasekar, Gothenburg, Sweden 2025

# List of Acronyms

| | |
|---|---|
| AC | Alternating Current |
| ACBD | Alternating Current Breakdown |
| ASTM | American Society for Testing and Materials |
| BD | Breakdown |
| CAD | Computer Aided Design |
| DC | Direct Current |
| DCBD | Direct Current Breakdown |
| EPDM | Ethlyne Propylene Diene Monomer |
| FEM | Finite Element Method |
| FGM | Field Grading Material |
| HVAC | High Voltage Alternating Current |
| HVDC | High Voltage Direct Current |
| HZ | Frequency |
| IEC | International Electrotechnical Commission |
| LIBD | Lightning Impulse Breakdown |
| MO | Mineral oil |
| r.m.s | Root Mean Square |
| s | seconds |
| SO | Silicone oil |
| UV | Ultra Violet |
| V | Voltage |
| XLPE | Cross-Linked Polyethylene |

# Contents

**List of Acronyms** **ix**

**List of Figures** **xiii**

**List of Tables** **xv**

**1 Introduction** **1**
1.1 Thesis work motivation . . . 1
1.2 Testing Voltages . . . 1
1.2.1 Testing with power frequency voltages . . . 2
1.2.2 Testing with Lightning Impulse voltages . . . 2
1.2.3 D.C voltages . . . 2

**2 Theoretical Background** **3**
2.1 Breakdown in solid dielectrics . . . 3
2.1.1 Intrinsic breakdown . . . 3
2.1.2 Streamer breakdown . . . 4
2.1.3 Edge breakdown . . . 4
2.2 Breakdown in liquids . . . 5
2.2.1 Electronic breakdown . . . 6
2.2.2 Suspended solid particle mechanism . . . 6
2.2.3 Cavity breakdown . . . 6
2.3 Weibull distribution . . . 6

**3 Development of the breakdown facility** **9**
3.1 Electrostatic fields and field stress control . . . 9
3.1.1 Electric field distribution and breakdown strength of Insulating materials . 9
3.1.2 Fields in homogeneous, isotropic materials . . . 10
3.1.2.1 Sphere to plane . . . 11

**4 Experimental details** **13**
4.1 Description of the material used . . . 13
4.1.1 Insulation(EPDM) . . . 13
4.1.2 FGM . . . 14
4.2 Preparation of the test specimen . . . 15
4.3 Description of the oil used . . . 15
4.3.1 Relative permittivity($\epsilon_r$),dielectric dissipation factor(Tan $\delta$) and DC resistivity . . . 15
4.3.2 AC breakdown testing on Insulating liquid . . . 15
4.3.3 Water content . . . 16
4.4 State of the art review of testing . . . 16
4.4.1 FEM Modelling . . . 16

4.5 Experimental setup . . . 17
4.5.1 AC breakdown test . . . 17
4.5.1.1 Short-time test . . . 17
4.5.2 DC breakdown test . . . 18
4.5.2.1 Test cell box . . . 18
4.5.2.2 Control Unit . . . 19
4.5.2.3 Moulded Electrode sample . . . 20
4.5.2.4 DCBD testing(short time test) . . . 21
4.5.2.5 DCBD testing with Electrode moulded sample . . . 21
4.5.3 Lightning Impulse test . . . 22
4.5.4 Swelling test . . . 23

**5 Experimental results and discussions** **25**
5.1 Swelling test . . . 25
5.1.1 Test with Mineral oil . . . 25
5.1.2 Test with Silicone oil . . . 27
5.2 Breakdown tests . . . 28
5.2.1 AC Breakdown test . . . 28
5.2.2 DC Breakdown test . . . 31
5.2.2.1 Moulded sample(short time test) . . . 33
5.2.2.2 Comparison of DCBD testing with moulded Electrode sample . . . 34
5.2.3 Lightning Impulse Breakdown test . . . 35

**6 Conclusion** **37**

**Bibliography** **39**

# List of Figures


2.1 Electrode arrangement used for measuring intrinsic breakdown in solids[1] . . . . . 4
2.2 Breakdown of solid specimen due to ambient discharge-edge effect [1] . . . . . 5

3.1 Rod-to-plane electrode configuration (with different field efficiency factor $\eta$ = V/dE$_{max}$)[1] . . . . . 10
3.2 Sphere-to-plane electrode system[1] . . . . . 11

4.1 AC Breakdown testing electrode setup[27] . . . . . 14
4.2 Cable joint design with a FGM later[33] . . . . . 15
4.3 AC Breakdown testing electrode setup . . . . . 16
4.4 (a) Electrode geometry for AC/DC dielectric testing (b) Triple point (c) Moulded electrode setup for Endurance test . . . . . 17
4.5 AC Breakdown testing for the material . . . . . 18
4.6 (a) Cell body(CAD model) (b) Cell dimension (c) Cell top(CAD model) (d) Cell top dimension (e) Test cell body (f) Test cell top . . . . . 18
4.7 DC Breakdown testing Connection setup . . . . . 19
4.8 Control Unit-LabVIEW . . . . . 19
4.9 (a) HV Electrode connect with top (b) Filled sample in the mould (c) Moulding placed in the press machine (d) Moulding in the press machine (e) Final output of moulded electrode sample . . . . . 20
4.10 (a) HV Electrode (b) Ground Electrode (c) DC source connection to the test cell (d) Connection to the test cell in the cage (e) Test cell with filled insulation oil . . 21
4.11 (a) HV Electrode (b) Ground Electrode (c) Test cell with moulded electrode connection . . . . . 22
4.12 LI Breakdown testing Connection setup . . . . . 22
4.13 LI Breakdown Testing Circuit[25] . . . . . 23
4.14 (a) Sample in the glass container (b) Diameter measurement (c) Weight machine (d) Thickness machine . . . . . 23

5.1 Swelling test on Insulation with Mineral oil(Mean value) . . . . . 26
5.2 Swelling test on FGM with Mineral oil(Mean value) . . . . . 26
5.3 Swelling test on Insulation(EPDM) with Silicone oil(Mean value) . . . . . 27
5.4 Swelling test on FGM with Silicone oil(Mean value) . . . . . 28
5.5 ACBD Testing (a) BD point on the HV electrode on FGM ;(b) BD point on the Ground electrode on FGM ;(c) BD point on the FGM sample;(d) BD point on the HV electrode on Insulation ;(e) BD point on the Ground electrode on Insulation ;(f) BD point on the Insulation sample . . . . . 29
5.6 ACBD testing:(a) Field distribution on FGM with mineral oil ;(b) Field distribution on FGM with Silicone oil;(c) Field distribution on Insulation with mineral oil; (d) Field distribution on Insulation with Silicone oil . . . . . 30
5.7 Weibull plots(normalized value) for AC breakdown testing on FGM with MO and SO . . . . . 31

5.8 Weibull plots(normalized value) for AC breakdown testing on Insulation(EPDM) with MO and SO . . . . . 31
5.9 DCBD Testing (a) BD point on the HV electrode on FGM ;(b) BD point on the Ground electrode on FGM ;(c) BD point on the FGM sample;(d) BD point on the HV electrode on Insulation ;(e) BD point on the Ground electrode on Insulation ;(f) BD point on the Insulation sample . . . . . 32
5.10 Weibull plots(normalized value) for DC breakdown testing on FGM with MO and SO . . . . . 33
5.11 Weibull plots(normalized value) for DC breakdown testing on Insulation(EPDM)) with MO and SO . . . . . 33
5.12 (a) HV electrode BD point (b) Ground electrode BD point (c) Moulded electrode sample (d) BD point on the moulded electrode sample . . . . . 34
5.13 Weibull plots(normalized value) for DC breakdown testing on FGM(comparison with Moulded sample) . . . . . 35
5.14 LIBD testing (a) BD point on the surface of the ground electrode on test 1 (b) BD point on the surface of the ground electrode on test 2 . . . . . 35
5.15 Simulation for the LIBD Testing(a) Electric field distribution with mineral oil (b) Electric field distribution with Silicone oil . . . . . 36
5.16 Weibull plots(normalized value) for LI breakdown testing on Insulation(EPDM) with MO and SO . . . . . 36

# List of Tables


4.1 Manufacturer of Insulation oil . . . . . 15
4.2 Dielectric parameters of Insulation oil according to IEC 60247 standards[17] . . . 15
4.3 AC Breakdown testing of Insulation oil according to IEC 60156 standards [21] . . 16
4.4 Water content of Insulation oil according to standard ASTM D6304-20[22] . . . . 16

5.1 Swelling test on Insulation(EPDM) with Mineral oil . . . . . 25
5.2 Swelling test on FGM with Mineral oil . . . . . 26
5.3 Swelling test on Insulation(EPDM) with Silicone oil . . . . . 27
5.4 Swelling test on FGM with Silicone oil . . . . . 28

# 1
# Introduction

NKT is one of the biggest company in the cable and cable accessories industry. Power cable accessories are an essential link in the power chain, connecting electricity transmission systems. The biggest sustainable electrical source like offshore wind farms are located far remote from the main users and one of the biggest challenges is how to transmit this high level of energy. Moreover, today DC is preferred over AC for transmitting electricity at high voltage over long distances because of lower losses. Based on this, NKT has huge motivation to develop HVDC products and for this, they should develop their lab facilities to have the opportunity to characterize the used materials.

One of the NKT's branches is located in Alingsås and in this branch, some of the cable accessories such as joint and termination for HVDC and HVAC are manufactured. NKT develops, produces and installs a full portfolio of high- and medium-voltage power cable accessories for use in offshore and onshore applications including power cable joints and terminations. Nowadays, there is a possibility to do certain small-scale tests, like dielectric spectroscopy, DC conductivity measurements, AC breakdown test, rheology test, and mechanical tests (tensile and tear strength), on rubber materials.

## 1.1 Thesis work motivation

The aim of the research project is to develop, build up and verify test cells to perform DC and lightning impulse breakdown testing on EPDM rubber materials and FGM used in cable accessories.
The two different test cell arrangements are necessary to enable short time and long-time breakdown testing. During short time testing (rapid rise test), the test samples can be placed in insulating liquid to avoid surface flashovers. The drawback of this method is that the insulating liquid might interfere with the rubber samples (swelling of the material). Therefore, such a test cell can only be used for short time tests and not for long time tests (endurance test).

## 1.2 Testing Voltages

Power systems equipment must be capable of withstanding both the rated voltage ($V_m$), representing the highest voltage of a specific system, and overvoltages. Consequently, it is imperative to conduct thorough testing of high-voltage equipment during its development phase and prior to commissioning. The magnitude and type of test voltage required varies depending on the rated voltage of the specific apparatus. Standard methods for measuring high voltages and fundamental techniques for application to all types of apparatus for alternating voltages, direct voltages, switching impulse voltages, and lightning impulse voltages are defined in the relevant national and international standards.

### 1.2.1 Testing with power frequency voltages

To evaluate the insulation capacity of the apparatus against the power frequency voltage of the system, a test will be conducted at either 50 Hz or 60 Hz. The test voltage is set at a level exceeding the anticipated operational voltage to replicate potential stresses over the equipment's service life. Indoor equipment tests are performed under dry conditions, while outdoor equipment may necessitate testing under standard rain conditions as outlined in the relevant standards.

### 1.2.2 Testing with Lightning Impulse voltages

Lightning strikes on transmission lines can generate high voltage surges that travel along the line, potentially causing damage to the system's insulation. These overvoltages can reach several thousand kilovolts, depending on the insulation. Extensive measurements and experience have shown that lightning overvoltages have a short duration, ranging from a fraction of a $\mu$sec to several tens of $\mu$sec before slowly decreasing. The standard impulse voltage is an aperiodic impulse that reaches its peak value in 1.2 $\mu$sec and then gradually decreases to half its peak value in about 50 $\mu$sec. Detailed information about the waveform of the standard impulse voltage and permitted tolerances is provided.

### 1.2.3 D.C voltages

In the past, direct current (DC) voltages were primarily used for scientific research. Industrial applications were mainly limited to testing cables with large capacitance, which require a high current when tested with alternating current (AC) voltages, and testing insulations where internal discharges could degrade the insulation under test[1]. However, with the increasing interest in high-voltage direct current (HVDC) transmission; testing in DC condition got important. Due to the lossess is less in the HVDC than the HVAC transmission. The DC voltage in the power systems that use only one electrical polarity for voltage or current. It also describes the constant, zero-frequency, or slowly varying average value of a voltage or current[56].

# 2

# Theoretical Background

The theoretical foundation of this work draws on insights and concepts from sources [1] and [51]. These references provide a framework that supports the analysis and arguments presented in this study work.

## 2.1 Breakdown in solid dielectrics

Solid insulation is an essential component of high-voltage equipment, providing mechanical support for conductive parts and insulating conductors from one another. The structure of insulation typically consists of a combination of solid, liquid, and gas materials. An ideal insulation material exhibits low dielectric loss and high mechanical strength, while also being free from gas and moisture. Additionally, good insulation materials demonstrate strong resistance to thermal and chemical compounds.

The breakdown of solid dielectrics is not solely determined by the applied voltage; it is also influenced by the duration for which the voltage is applied. Several factors affect the dielectric strength of solid insulation materials, including ambient temperature, humidity, test duration, impurities, the type of voltage applied (AC, DC, or impulse), and the pressure applied to the test electrodes.

The different breakdown mechanisms for solid dielectric materials are

1. Intrinsic breakdown
2. Streamer breakdown
3. Electromechanical breakdown
4. Edge breakdown
5. Thermal breakdown
6. Erosion breakdown
7. Tracing

In this project, we conducted detailed observations and analyses of various breakdown mechanisms, outlining their characteristics and functions as follows.

### 2.1.1 Intrinsic breakdown

It is crucial to ensure that the dielectric material is pure and uniform by controlling the temperature and environmental conditions during testing. The sample should be subjected to stress during testing to prevent external flashover. When voltage is applied for a specific duration, the electric strength increases rapidly until it reaches its maximum limit, referred to as intrinsic electric strength. This strength is influenced by the material and the temperature conditions. In the experimental conditions, the center of the sample should be subjected to stress for testing,

while the edges should experience less stress to prevent discharge in the medium, as illustrated in Figure 2.1.

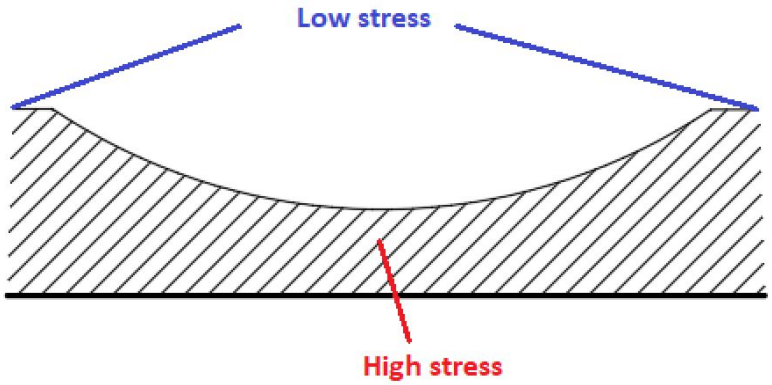


**Figure 2.1:** Electrode arrangement used for measuring intrinsic breakdown in solids[1]

The Intrinsic strength occurs when electrons in the insulator gain enough energy from the applied field to cross the forbidden gap from the valence band to the conduction band. In pure homogeneous dielectric materials, the conduction band and valence band have a significant energy gap between them, and at room temperature, electrons do not have enough thermal energy to move from the valence band to the conduction band. In perfect dielectrics, the conductivity is zero. In practice, missing atoms and the presence of impurities lead to imperfections in the crystal structure. The impurity atoms can serve as traps for free electrons in energy levels just below the conduction band.

### 2.1.2 Streamer breakdown

Under uniform field conditions, conduction electrons gain enough energy from a critical electric field to liberate themselves from the lattice atoms through collisions, leading to breakdown[1,2]. Breakdown occurs when the electrodes are placed in the specimen, creating an electron avalanche that bridges the gap between the electrodes. when an electron in the dielctric begins its drift from the cathode towards the anode due to the applied electric field, it acquires enrgy. During its motion,the electron undergoes various collisions which cause it ot lose some of that energy. If the mean free path is sufficient long, the electron's energy gain can surpass the ionization energy of the lattice. This results in the excitation of a lattice atom, leading to the release of an additional free electron upon collision.

The strength of the chain is defined by its weakest link, and in polymers, covalent bonds are sensitive to ionizing radiation. When an electron's energy exceeds the lattice ionization potential, it can cause the liberation of an additional electron through collision, resulting in the formation of an electron avalanche. Avalanche reaches a critical size leads to breakdown. In practice, breakdown doesn't occur due to a single avalanche; rather, it is caused by the formation of multiple avalanche events within the dielectric material. These avalanches propagate through the entire thickness of the material, contributing to the overall breakdown process.

### 2.1.3 Edge breakdown

In practical Insulation systems, solid materials consistently experience stress alongside one or more other materials. When one of these materials is a gas or a liquid, it si the weaker medium that exerts a more significant influence on the measured breakdown voltage, rather than the solid material itself.

The cross section of the dielectric layer between sphere-plane electrodes is shown in the Figure 3.2

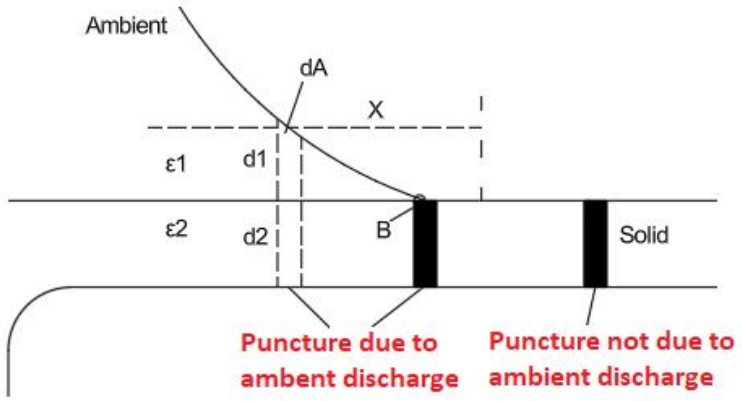


**Figure 2.2:** Breakdown of solid specimen due to ambient discharge-edge effect [1]

Assuming a homogeneous field and ignoring the field distribution, we can focus on an elementary cylindrical volume with area dA spanning the electrodes at distance x. Upon applying the voltage V between the electrodes, a fraction $V_1$ of the voltage appears, where d1 and d2 represent the thickness of the media 1 and 2 in Figure 2.2, and $\epsilon_1$ and $\epsilon_2$ are their respective permittivities.

$$V_1 = \frac{V d_1}{d_1 + \left(\frac{\varepsilon_1}{\varepsilon_2}\right) d_2} \tag{2.1}$$

In this section, where a gaseous dielectric is connected in series with a solid dielectric and is subjected to stress between two parallel plate electrodes, the stress in the gaseous part will exceed that of the solid part by the ratio of permittivities, $\varepsilon_s = \frac{\varepsilon_2}{\varepsilon_1}$ or $E_1 = \varepsilon_s E_2$. In the scenario depicted in Figure 2.2, the stress in the gaseous part increases as x decreases, reaching very high values as $d_1$ becomes very small (point B in Figure 2.2). Consequently, the surrounding medium breaks down at a relatively low applied voltage. The charge at the tip of the discharge further disrupts the local field and transforms the arrangement into a highly non-uniform system. The charge concentration at the tip of a discharge channel has been estimated to be sufficient to produce a local field, which is higher than the intrinsic breakdown field. A local breakdown at the tips of the discharge is likely, and as a result of many such breakdown channels forming in the solid and progressively extending through the entire thickness, a complete breakdown occurs[1].

## 2.2 Breakdown in liquids

The electrical breakdown of liquids is less advanced compared to that of gases and solids. There are two primary theories that explain this phenomenon. The first theory focuses on avalanche ionization, which occurs when electrons collide with atoms in the presence of an applied electric field, leading to ionization. The second theory highlights the role of foreign particles within liquid insulation, as their presence significantly influences the liquid breakdown strength. These particles are polarizable and possess a higher permittivity than the liquid, causing electrical forces that attract them to aread of maximum stress. Furthermore, impurities can also appear as gaseous bubbles, which have a lower breakdown strength than the surrounding liquid. In such cases, the breakdown of these bubbles has the potential to instigate a complete breakdown of the liquid[3].

### 2.2.1 Electronic breakdown

The current observed at the cathode is thought to originate from a combination of field emission and field-enhanced thermionic emission. Despite this potential dual mechanism, breakdown measurements across a broad temperature spectrum reveal minimal temperature dependence. This suggests that the predominant emission process at the cathode likely leans more towards field emission process at the cathode likely leans more towards field emission than thermionic emission. Additionally, the reintroduction of positive ions and positively charged contaminants to the cathode surface could contribute to local electric field enhancements, which may facilitate localized electron emission.

when and electron is injected into the liquid, it gain more energy from this field than they lose during collisions with molecules. These energized electrons are accelerated until they have sufficient energy to ionize molecules upon collision, which initiates an avalanche effect. The initial avalanche occurs when the increase in energy of an electron over the distance it travels between collisions meets or exceeds the energy required to ionize a molecule[3].

$$eE\lambda = ch\nu \tag{2.2}$$

where E represents the applied field, $\lambda$ represents the electron mean free path, h$\nu$ denotes the quantum of energy lost in ionizing the molecule, and c is an arbitrary constant.

### 2.2.2 Suspended solid particle mechanism

Solid impurities can appear in liquids as fibers or small particles. When an electric field is applied, these particles become charged and feel a force that moves them toward the strongest part of the field. If the particles have a higher permittivity than the liquid around them, they will cause more electric flux to gather at their surfaces. This gathering attracts other particles to the area with higher flux, making them align form head to tail and form a bridge across the gap. The electric field in the liquid between the particles becomes stronger, and if it exceeds a certain level, it can lead to a breakdown.

### 2.2.3 Cavity breakdown

Insulating liquids may contain gaseous inclusions in the form of bubbles. The formation of these bubbles can occur due to several factors, including the presence of gas pockets on the electrode surface, fluctuations in temperature and pressure, and the vaporization of the liquid as a result of corona discharge originating from points and irregularities on the electrode. The initial size of the bubble is assumed to elongate under the influence of the field and is affected by external pressure and temperature[5].

## 2.3 Weibull distribution

Weibull models are utilized to describe various types of observed component failures and phenomena. They are commonly applied in reliability and survival analysis. In addition to the traditional two-parameter and three-parameter Weibull distributions found in reliability and statistics literature, many other Weibull-related distributions are also available[35].

This comprehensive review delves into a variety of statistical methods employed to assess the insulation characteristics of solid insulating materials[24]. The experimental results highlighted throughout this discussion reveal that the probability of breakdown at a given test voltage is

significantly influenced by several factors, including the specific testing method utilized, the parameters associated with that method, and the inherent attributes of the breakdown probability function itself.

Furthermore, the review outlines the application of these statistical methods in establishing critical metrics such as insulation strength and material longevity. A particular focus is placed on the Weibull distribution, which is commonly used to analyze and interpret breakdown data. This statistical approach allows for a nuanced understanding of failure rates and reliability over time.

It is important to emphasize the need for careful interpretation of the results obtained from statistical tests, as low-breakdown-probability test methods introduce a level of variability that can affect the findings. The discussion also includes test results that explore different electrode geometries, providing insights into how these configurations impact insulation performance. Additionally, samples with varying dielectric properties are examined, along with an analysis of two distinct types of insulation liquids, further enriching our understanding of how these factors interplay in the context of insulating materials.

The Weibull plot is an essential tool for analyzing dielectric breakdown results, particularly in understanding the reliability and failure mechanisms of solid materials under electrical stress[54]. By displaying failure probabilities as a function of breakdown voltage on a logarithmic scale, the Weibull distribution provides valuable insights into the statistical behavior of dielectric materials.

The scale parameter ($\alpha$) represents the breakdown voltage at a 63.2% probability of failure, serving as a benchmark for comparing the durability of different samples or conditions. Conversely, the shape parameter ($\beta$) indicates the variability of breakdown voltages, with higher values indicating more uniform material properties[54].

This method allows researchers to differentiate between intrinsic and extrinsic breakdown mechanisms. Intrinsic breakdowns typically exhibit higher $\alpha$ values, reflecting consistent and predictable material performance[2.1.1]. In contrast, extrinsic breakdowns, often caused by manufacturing defects or contaminants, show greater variability.

Additionally, Weibull analysis aids in extrapolating long-term performance from short-term tests by correlating breakdown voltage distributions with stress levels[54].

# 3

# Development of the breakdown facility

This section is referred from the concepts from sources [1] and [51]. These references provide a supports the analysis.

## 3.1 Electrostatic fields and field stress control

In response to the growing need for electrical energy, transmission level voltages have significantly increased over the last few decades. As a result, designers are required to minimize the size and weight of electrical equipment to stay competitive. Achieving this goal depends on a comprehensive understanding of insulating materials, as well as knowledge of electric fields and methods for controlling electric stress[10,11,12,13].

The majority of issues related to the electrical insulation of high direct, alternating, and impulse voltages are connected to electrostatic and occasionally electrical conduction fields. It is important to note, however, that the allowable field strengths in the materials are dependent on the electrostatic field distributions. As a result, these issues can become extremely challenging to resolve.

### 3.1.1 Electric field distribution and breakdown strength of Insulating materials

The concept of achieving effective insulation between two electrodes is discussed. The breakdown strength ($E_b$) of the homogeneous insulation material be placed in between the electrodes. The distance (d) between the electrodes can be calculated by using the formula d=V/$E_b$ where V is the voltage applied to the electrode. The maximum electric field distribution ($E_{max}$) occurs at the tip of the electrode.
The electrode arrangement consists of a rod and plane, insulated by air and maintained under atmospheric pressure. The length of the gap and the density of the air remain unchanged, while the diameter D of the rod will vary, as shown by the dotted line in the Figure 3.1.

The maximum field strength $E_{max}$ at the rod tip and the mean field strength value $E_{mean}$=V/d. Additionally, a "field efficiency factor" ($\eta$) is defined based on these two quantities.

$$\eta = \frac{E_{mean}}{E_{max}} = \frac{V}{dE_{max}} \tag{3.1}$$

If the breakdown of the gap is exclusively due to $E_{max}(E_b = E_{\max})$, we can calculate the breakdown voltage $V_b$ using Equation 3.1.

$$V_b = E_{\max} \times d \times \eta = E_b \times d \times \eta \quad (\text{with } E_b = E_{\max}) \tag{3.2}$$

Equation 3.2 explains the electric field factor $\eta$, which helps understand the electric field distribution between electrode configurations[1].

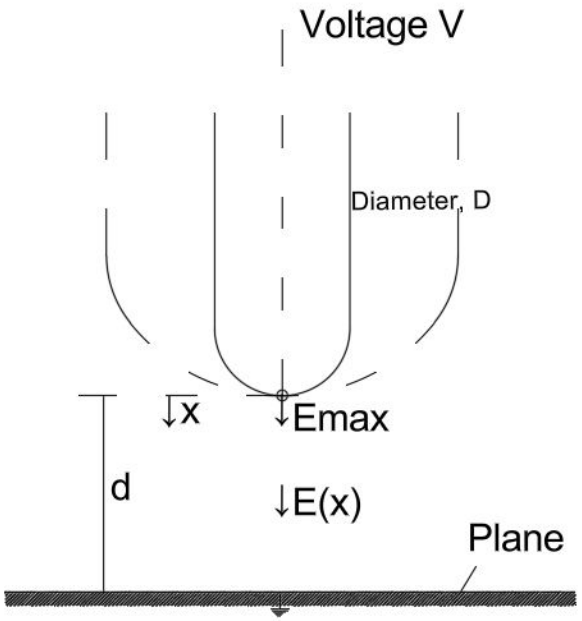


**Figure 3.1:** Rod-to-plane electrode configuration (with different field efficiency factor $\eta = V/dE_{max}$)[1]

In practice, the dielectric stresses experienced by insulation materials in high voltage apparatus are determined through field analysis. It has been consistently observed that breakdown stresses depend on the field distribution within region of high electrical stress. As a result, models that focus solely on these high stress areas are typically sufficient, providing notable advantages. This approach streamlines the design of experimental insulation assemblies, thus reducing both time and costs. Furthermore, it enables a considerable decrease in the necessary voltage levels by minimizing the mode size, achieved through electrode configurations that deliberately omit low field regions.

### 3.1.2 Fields in homogeneous, isotropic materials

The influence of electrical conductivity on field distribution may be ignored for most insulating materials stressed by alternating voltages above 1 Hz. Simple electrostatic field theory can be applied to practical applications involving power frequency or impulse voltages. However, conduction phenomena can impede electrostatic field theory with direct or slowly alternating voltages. In the extreme case, the field is purely given by conduction, and the relationship between field strength and current density J is $J = \sigma E$, where $\sigma$ is the electrical conductivity.

The electrical conductivity $\sigma$ is subject to change over time due to relaxation phenomena and being influenced by temperature and field intensity. This issue is highlighted here to underscore the challenges encountered in DC voltage applications. The following examples of electrostatic field distributions represent those found in high-voltage power cables and the electrodes utilized for dielectric strength testing.

#### 3.1.2.1 Sphere to plane

The sphere to plane electrode configuration is used to study dielectrics near breakdown voltage, providing maximum field intensity at the point of contact with a gradual decrease away from it. the field lines are not perfectly parallel to the axis of symmetry, for a sufficiently large sphere radius and small gap, the approximation can be accurate as a uniform field ($\eta = 1$), enabling the calculation of field intensity similar to the case of parallel plane geometry E = V/d. A schematic representation of the sphere-to-plane electrode system is presented in Figure 3.2.

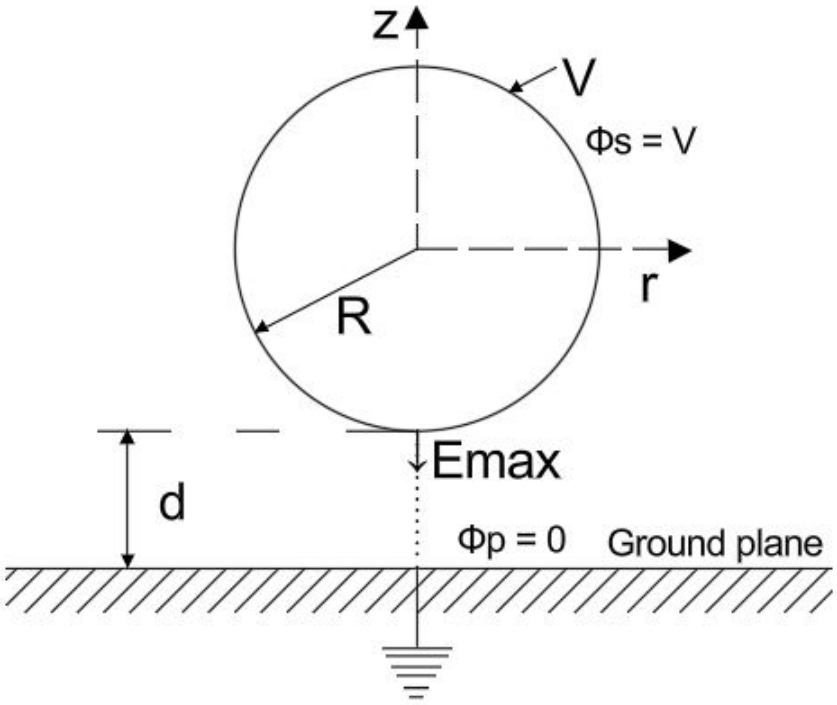


**Figure 3.2:** Sphere-to-plane electrode system[1]

Investigation of the electrostatic field, potential, and capacitance of a sphere-to-plane electrode system are discussed in multiple scholarly publications [15-16]. The field distribution can be determined analytically by applying the method of charges [1]. The field pattern and the potential distribution for the electrode system are analogous to those generated by two-point charges. The approximation for the maximum field strength, denoted as "$E_{max}$," is derived from the image charge technique, as demonstrated in Equation 3.3.

$$E_{max} = 0.9\frac{V}{d}\frac{R+d}{R} \tag{3.3}$$

Where d is the shortest distance between the electrodes, R is the radius of the sphere electrode, and V is the applied voltage to the electrode.

# 4

# Experimental details

## 4.1 Description of the material used

The use of DC cables to transport electricity, particularly over long distances, has become increasingly important in recent years. However, as the length of the cable line increases, so does the number of joints needed to connect the cable segments. These cable joints must perform the same functions as the cables they link and should have a lifespan at least equal to that of the cables. Unfortunately, cable joints are often the weakest links in cable systems, with approximately 70% of damage to cable lines attributed to failures in joints and terminations. This vulnerability arises from the interfaces between the subcomponents of the joints, where harmful physico-chemical phenomena can occur, as well as from high operational stresses that may result from improper manufacturing or installation. Additionally, contamination during assembly can further compromise the integrity of the joints[26].

In this thesis two types of materials are investigated: EPDM and FGM.

### 4.1.1 Insulation(EPDM)

Ethylene-propylene rubber, commonly known as EPM and EPDM, is one of the most widely used and rapidly growing synthetic rubbers, suitable for both specialty and general-purpose applications. Current polymerization and catalyst technologies enable the design of polymers that meet specific and demanding application and processing requirements[55].The versatility in polymer design and heat resistance has led to a wide range of rubber applications, including electrical insulation, jacketing for low and medium voltage connectors, and tapes. Ethylene-propylene copolymers display elastomeric properties across a broad range of compositions. The ethylene content of commercial EPDM polymers typically ranges from 45% to 80% by weight. Below 45% ethylene content, the drop in properties makes the material less suitable for industrial applications[55].

EPDM is widely used as an insulation material in High voltage cable system, due to its excellent dielectric and thermal-mechanical properties, making it ideal for reinforcing insulation in cable accessories[36]. In the multi-layer structure of cable accessories, which is the most vulnerable component in power transmission cable systems, a significant difference in electrical conductivity between two adjacent dielectric layers can lead to electric field distortion.[37,38].

The ratio of ethylene to propylene in the elastomer is a key factor that influences the glass transition temperature of the material. Ethylene-propylene rubber vulcanizates possess several important properties, including excellent heat resistance, a wide range of tensile strength and hardness, outstanding electrical resistance, and good chemical resistance, particularly to polar media, as well as resistance to moisture and steam[55].

### 4.1.2 FGM

In cable joints, that we can seen in the figure 4.1, where the external semiconductive screen of the insulation is removed, the equipotential lines are closely spaced. This indicates the presence of a strong electric field[27] in that area. Consequently, it is crucial to design cable joint configurations and select materials—known as stress-control materials—that effectively manage the electric field throughout the insulation layer[28] of the cable joint. Electric field control methods can be classified into two primary categories: a) Capacitive field grading,(which encompasses approaches such as geometrical electrode grading (employing conductive components with appropriately designed shapes), refractive grading (utilizing materials with high permittivity[27,29]), and condenser grading (integrating metallic elements)) and b) Resistive field grading (which utilizes materials that possess suitable current field characteristics, referred to as field grading materials (FGM). The behavior of the electric field grading is influenced by whether capacitive or resistive current predominates).

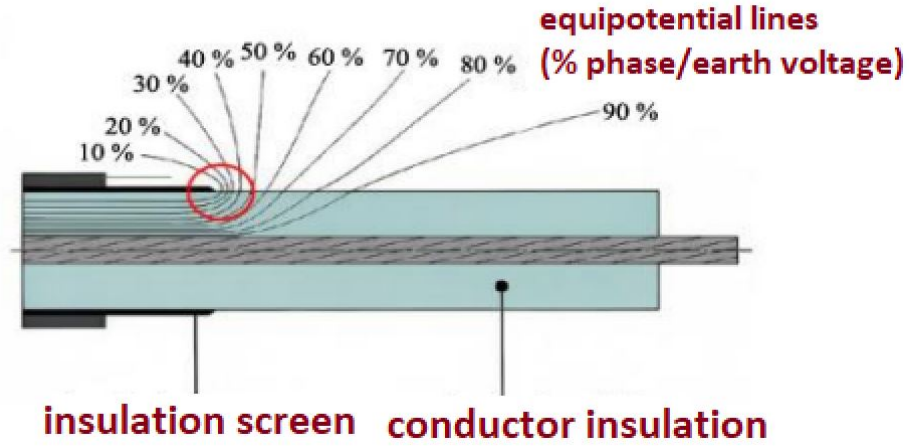


**Figure 4.1:** AC Breakdown testing electrode setup[27]

The materials used to control the electric field can be categorized as either capacitive or resistive, depending on whether the capacitive(respectively resistive) contribution to the current is greater than the resistive(respectively capacitive) one[30]. Generally, these materials exhibit a nonlinear relationship between permittivity (or conductivity) with respect to both the electric field and temperature[34].

In cable joints, field grading materials (FGM) with strong non-linear, field-dependent conductivities can be used. These materials are composed of polymeric composites, such as silicone rubbers, ethylene propylene rubbers (EPR), or ethylene propylene diene monomer rubbers (EPDM), combined with fillers like zinc oxide (ZnO) or silicon carbide (SiC) [31-32]. A model of a joint with a FGM layer in the HVDC joint is shown in Figure 4.2 [33]. An analysis of the impact of FGM on the electric field in a cable joint model is discussed in [31], which indicates that resistive field grading is associated with space charge formation. However, the influence of temperature on this phenomenon has not been analyzed, and the values of the surface space charge at the interfaces between the cable insulation and the joint[34].

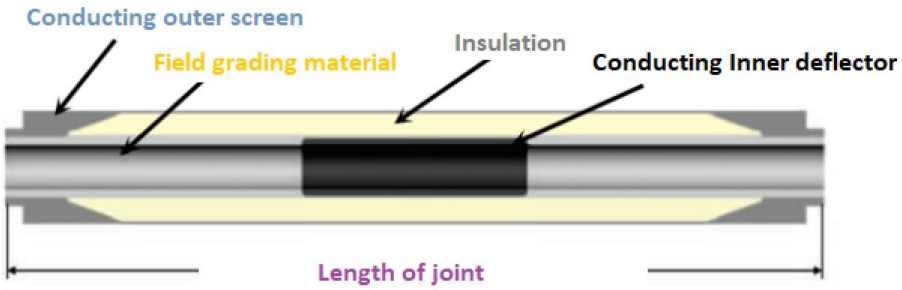


**Figure 4.2:** Cable joint design with a FGM later[33]

## 4.2 Preparation of the test specimen

The plaque sample, with a thickness of 1 mm, is manufactured using a pressing machine at a temperature of 165°C and a pressure of 200 bar for a duration of 30 minutes. Five round test objects of 60 mm diameter can be punched from one plaque sample.

## 4.3 Description of the oil used

Insulating oils serve as a surrounding medium to prevent flashover during dielectric testing. Mineral oil and silicone oil are commonly employed for this testing. The viscosity of silicone oil is higher than that of mineral oil. The manufacturer of the insulating liquid is outlined in the following Table 4.1.

**Table 4.1:** Manufacturer of Insulation oil

| Oil | Manufacturer | Type |
|---|---|---|
| Mineral oil | Shell diala | S4 ZX-I |
| Silicone oil | Wacker | AP100 |

### 4.3.1 Relative permittivity($\epsilon_r$),dielectric dissipation factor(Tan $\delta$) and DC resistivity

The tests are conducted following IEC 60247 standards[17], with some variations in the cleaning procedure. A 1 kV AC voltage is used to measure tan $\delta$ and relative permittivity, while a 500 V DC voltage is applied for resistivity measurement. The test cell has an electrode spacing of 2 mm, creating an electrical stress of 250 V/mm for DC resistivity measurement, as per the standard recommendation. All tests are carried out at a temperature of 90°C.
The dielectric parameters for the insulation liquid are presented in the Table 4.2.

**Table 4.2:** Dielectric parameters of Insulation oil according to IEC 60247 standards[17]

| Oil | Tan $\delta$ (%) | Relative permittivity | Volume resistivity(ohm-m) | DC Conductivity(S/m) |
|---|---|---|---|---|
| Mineral oil | 0.05 | 2 | $1.19\times10^{+}12$ | $8.37\times10^{-}13$ |
| Silicone oil | 0.018 | 3 | $1.96\times10^{+}12$ | $5.09\times10^{-}13$ |

### 4.3.2 AC breakdown testing on Insulating liquid

The dielectric strength of insulating liquids is determined by gradually increasing the applied voltage in line with the IEC 60156 standard[21] until electrical breakdown occurs in the gap

between the electrodes. The distance between the electrodes must be adjusted to 2.5 mm. Perform six breakdown tests on the same cell filling, allowing a pause of at least 2 minutes between each test before reapplying the voltage. Ensure that no gas bubbles are present within the electrode gap. Record the resulting values in kilovolts. According to the standard, BD traces must be removed from the electrode gap through magnetic or manual stirring and the tested value is presented in the Table 4.3 and the electrode can be seen in the following Figure 4.3.

**Figure 4.3:** AC Breakdown testing electrode setup

**Table 4.3:** AC Breakdown testing of Insulation oil according to IEC 60156 standards [21]

| Oil | Breakdown voltage(kV) |
|---|---|
| Mineral oil | 97.03 |
| Silicone oil | 78.86 |

### 4.3.3 Water content

The water content for the insulating oil needs to be determined according to standard ASTM D6304-20[22], and the test results are shown in the following Table 4.4.

**Table 4.4:** Water content of Insulation oil according to standard ASTM D6304-20[22]

| Oil | Water content(ppm) |
|---|---|
| Mineral oil | 1.3 |
| Silicone oil | 71 |

## 4.4 State of the art review of testing

### 4.4.1 FEM Modelling

The electric field simulations were carried out using COMSOL Multiphysics. This model features an asymmetric, two-dimensional geometry that utilizes electric current interfaces from the COMSOL AC/DC module. The dimensions of the electrodes are designed in accordance with IEC standards 60243-1[18]. The triple point, illustrated in the Figure 4.4(b), results in a high concentration of the electric field, which can cause punctures and breakdowns in the sample.

The semispherical high-voltage electrode is specifically designed for endurance tests to effectively manage the electric field at the electrode's center. Furthermore, the ground electrode incorporates sharp edges to mitigate the formation of a triple point on the ground side that illustated in the Figure 4.4(c), thereby better controlling electric field concentration.

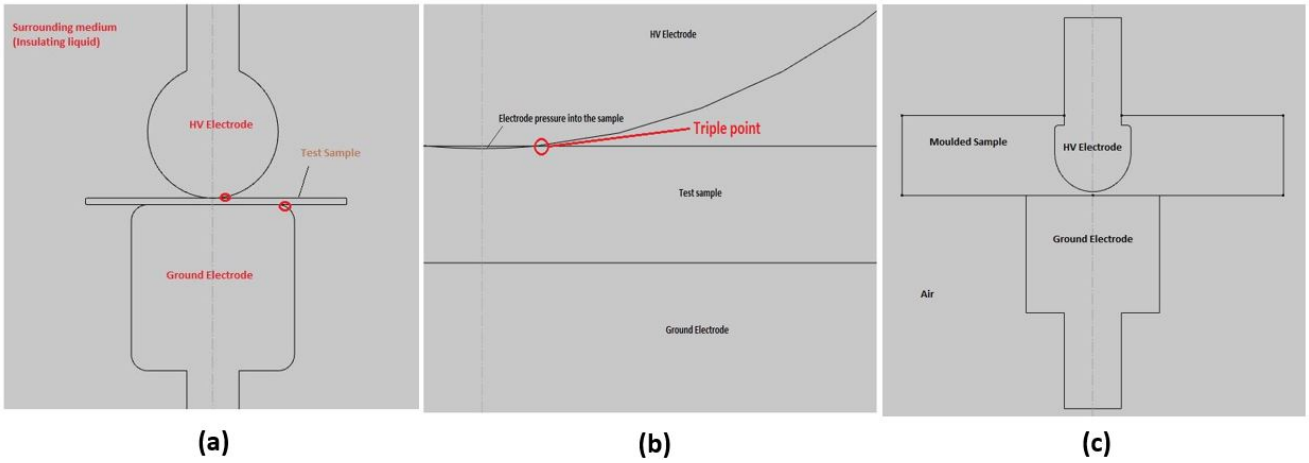


**Figure 4.4:** (a) Electrode geometry for AC/DC dielectric testing (b) Triple point (c) Moulded electrode setup for Endurance test

## 4.5 Experimental setup

### 4.5.1 AC breakdown test

The voltage values are recorded as equivalent r.m.s. values. It is recommended to utilize a peak reading voltmeter and then divide the obtained reading by $\sqrt{2}$. The total error of the voltage-measuring circuit should not exceed 5% of the measured value, which includes the error due to the response time of the voltmeter. The response-time induced error should not surpass 1% of the breakdown voltage at any rate of rise used. The sphere electrode is utilized as a high voltage point with a 20 mm diameter, while the cylindrical electrodes function as the ground with a 25 mm diameter on each side. The specified corner radius for the electrode is 2.5 mm as per the IEC 60243-1 standards[18] and the test cell setup for the AC Breakdown testing is depicted in the Figure 4.5.

#### 4.5.1.1 Short-time test

The rate of voltage rise is 500 V/s for FGM and 2 kV/s for the insulation material accordance with IEC 60243-1 standards[18].

**Figure 4.5:** AC Breakdown testing for the material

### 4.5.2 DC breakdown test

The DC dielectric breakdown testing was conducted on the sample using two different insulating oils as a surrounding medium to prevent surface flashover, in accordance with IEC standards 60243-2[19].

#### 4.5.2.1 Test cell box

The test cell box is constructed from plexiglass, also known as acrylic glass or polymethyl methacrylate. This material is transparent and rigid, with excellent electrical insulating properties due to its high resistivity and low electrical conductivity. The dimensions of the test cell box are shown in the Figure 4.6.

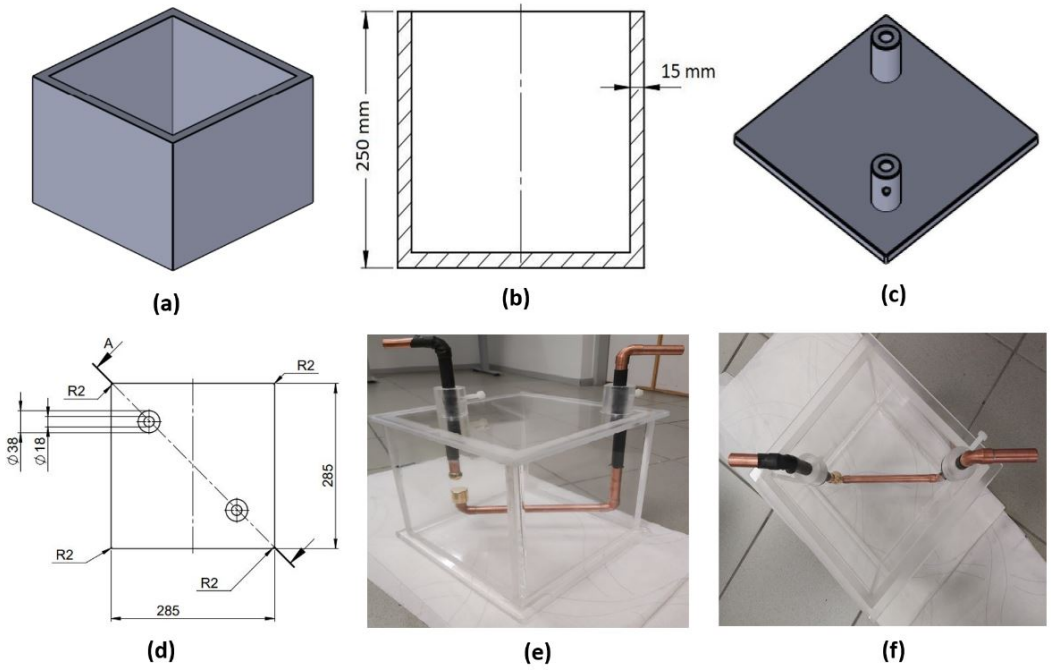


**Figure 4.6:** (a) Cell body(CAD model) (b) Cell dimension (c) Cell top(CAD model) (d) Cell top dimension (e) Test cell body (f) Test cell top

The copper rod has a diameter of 16 mm and is used to connect the high voltage and ground connections. It is covered with heat shrink for extra safety to prevent flashovers. The top part is removable and has two bushings with plastic screws for adjusting the rod to place the testing object.
The test cell is filled with insulating liquid of around 7 liters to cover the electrode to avoid flashover during the test. The distance between the high-voltage and ground rod is designed as 200 mm to prevent surface flashover. The block diagram for the Test setup is shown in the Figure 4.7.

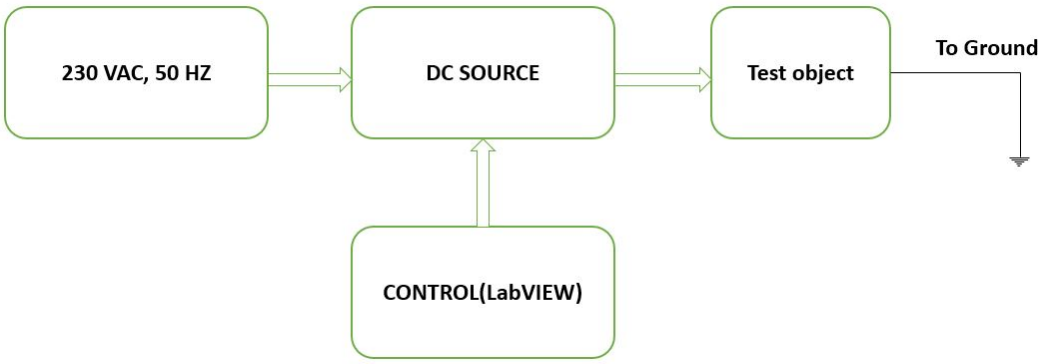


**Figure 4.7:** DC Breakdown testing Connection setup

#### 4.5.2.2 Control Unit

The control unit manages the DC source, applying voltage and recording the results. For this test, LabVIEW is used as the control unit. LabVIEW is a versatile tool that enables engineers and scientists to design, develop, and deploy sophisticated measurement, testing, and control systems.

The program has been developed and implemented with assistance from an external source, and the front panel, shown in the Figure 4.8, displays the port options and it includes settings for the voltage setpoint (both start and end) measured in kilovolts (kV), the ramping rate (in kV/sec), and the maximum current configuration for the test. Additionally, the elapsed time feature captures the duration of the breakdown, while the graph tracks and records the breakdown throughout the test.

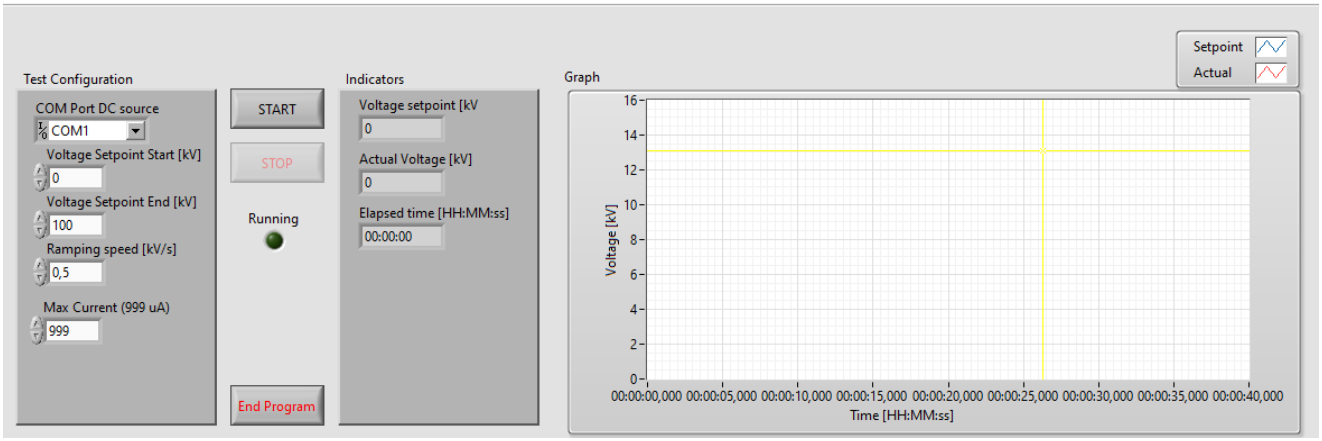


**Figure 4.8:** Control Unit-LabVIEW

#### 4.5.2.3 Moulded Electrode sample

The moulded sample, which was produced using a FGM combined with a high-voltage (HV) electrode, is illustrated in the accompanying Figure 4.9. This process involved carefully controlling the parameters of the moulding technique to ensure optimal integration of the materials. In long-term tests, samples with surrounding media are not possible due to the effects of oil swelling (absorbed or desorbed) in the sample. The triple point is also eliminated due to the design (removing insulating oil), that we can observed in the Figure 5.13.

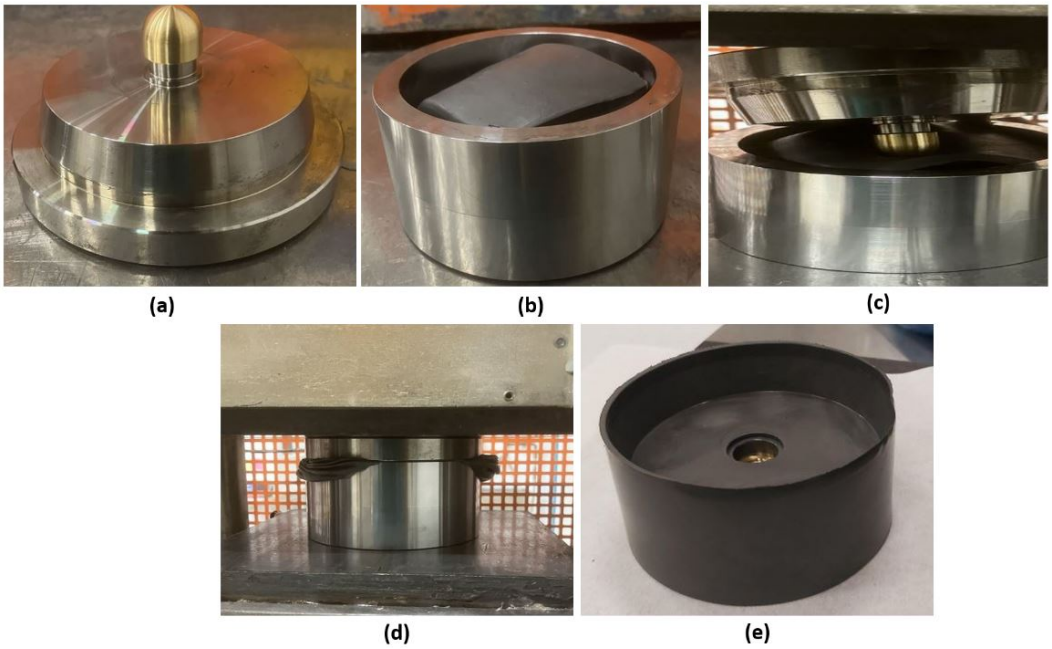


**Figure 4.9:** (a) HV Electrode connect with top (b) Filled sample in the mould (c) Moulding placed in the press machine (d) Moulding in the press machine (e) Final output of moulded electrode sample

The moulding process for the HV electrode is designed to have a sample thickness of 1mm at the tip of the electrode.

Once the mould is filled, the sample is precisely formed using a hydraulic press machine. The pressing process takes place at a controlled temperature of 165°C, which is essential for achieving the desired material properties. The mold is subjected to a pressure of 200 bar, allowing for efficient shaping and compaction of the sample. This process is maintained for a duration of 30 minutes to ensure thorough curing and adherence of the material.

#### 4.5.2.4 DCBD testing(short time test)

The short-duration test is designed to assess the performance characteristics of EPDM and FGM rubber compounds.The five rounded objects were punched out from a plaque sample that was prepared from the mould.

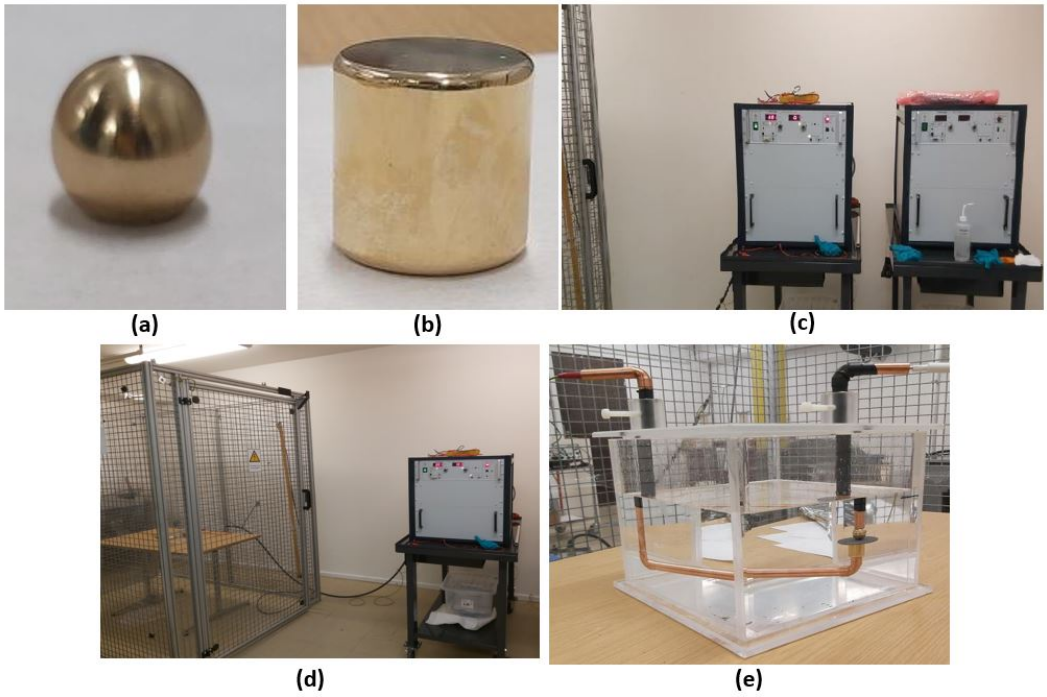


**Figure 4.10:** (a) HV Electrode (b) Ground Electrode (c) DC source connection to the test cell (d) Connection to the test cell in the cage (e) Test cell with filled insulation oil

The experiment takes place within a designed test cell that can shown in the Figure 4.10, which allows for controlled conditions and accurate measurements throughout the evaluation process. The surrounding mediums used in these tests include mineral oil and silicone oil, to avoid the surface flashover during the test, because of high dielectric strength and low viscosity.

By immersing the rubber material in these oils, the study aims to explore factors such as swelling, degradation, and overall durability during long time tests.

#### 4.5.2.5 DCBD testing with Electrode moulded sample

The sample with the molded electrode is designed to eliminate the triple point and access the dielectric strength of the material. This involves applying a ramping mode of direct current (DC) voltage to the sample, which is tested without the presence of any surrounding medium. This approach allows for a more accurate examination of the material's intrinsic properties under electrical stress, providing valuable data on its performance and reliability for various applications.

The high voltage (HV) electrode(smooth surface tapered shape at the end, which effectively concentrates the electric field at the center of the electrode) and the ground electrode were utilized in the endurance test, which measures the material's ability to withstand electrical stress over time. Both components and the test setup are illustrated in the accompanying Figure 4.11, providing a clear visual representation of the configuration used in the experiments.

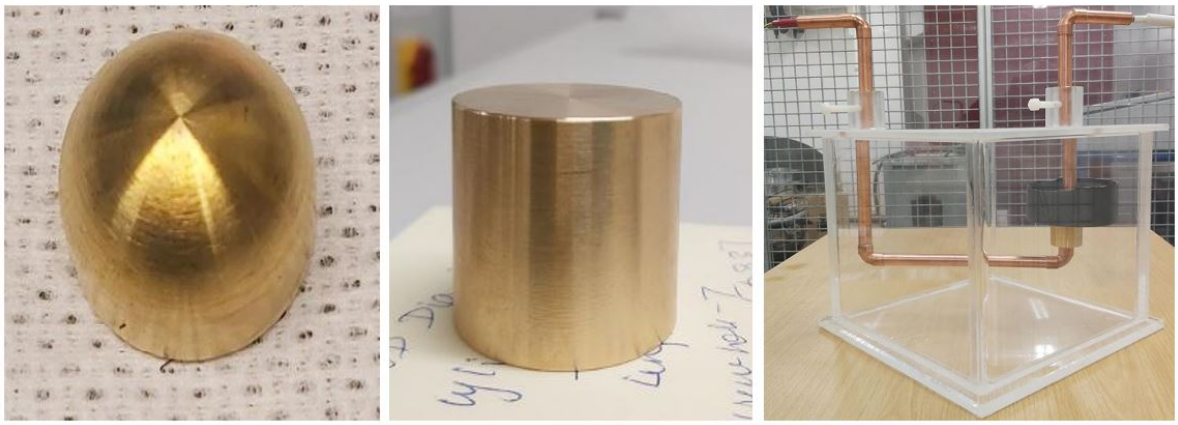


**Figure 4.11:** (a) HV Electrode (b) Ground Electrode (c) Test cell with moulded electrode connection

### 4.5.3 Lightning Impulse test

The LIBD testing was conducted on insulation material.The minimum voltage applied using the impulse generator is 30 kV. If the breakdown occurs below this level, the waveform cannot be tracked in data acquisition. Therefore, LIBD testing was not performed on the FGM in this test.Test conducted with two different insulating oils as a surrounding medium to prevent surface flashover, in accordance with IEC 60243-3 standards[20].

The Figure 4.12 illustrates the connection for the Lightning Impulse testing.

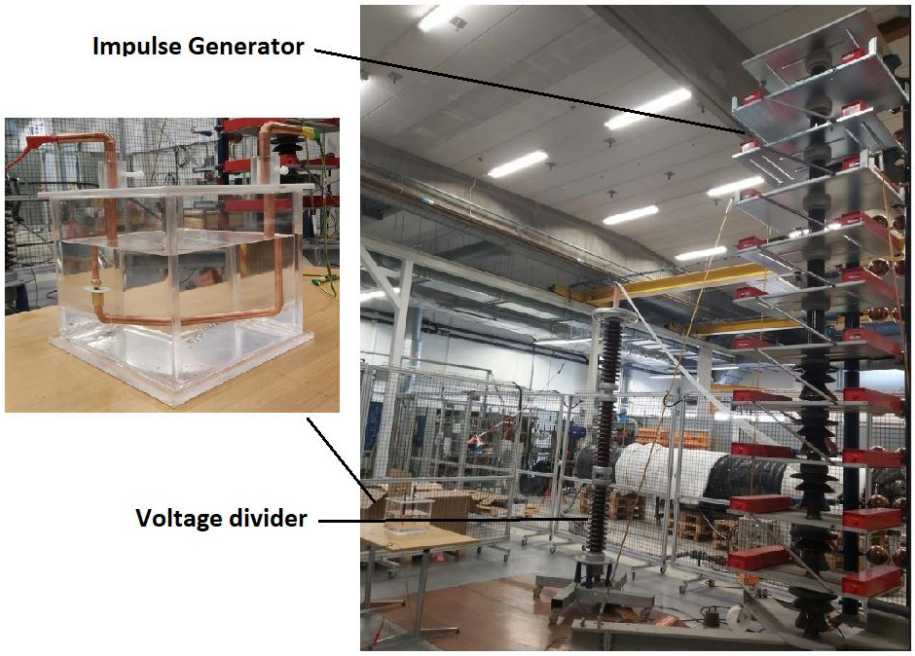


**Figure 4.12:** LI Breakdown testing Connection setup

The test circuit utilized in the LI breakdown testing is depicted in the Figure 4.13.

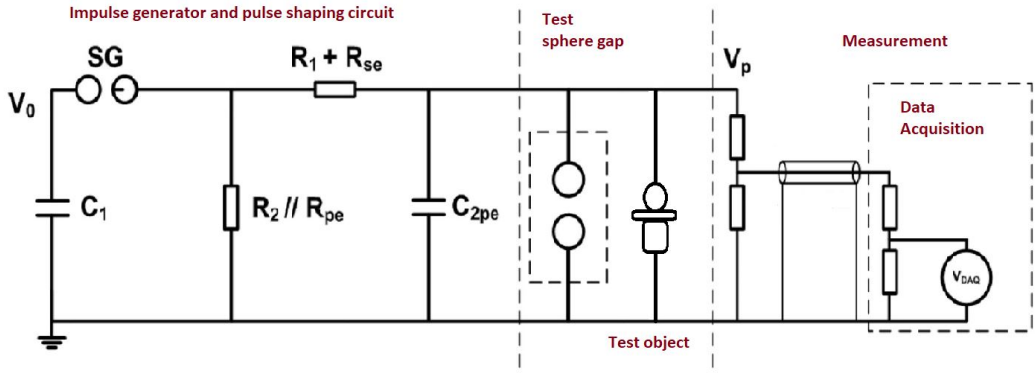


**Figure 4.13:** LI Breakdown Testing Circuit[25]

### 4.5.4 Swelling test

It is understood that the presence of small amounts of hydrophilic impurities in the rubber material significantly influences their oil absorption and desorption behavior[52,53]. To investigate this, a model of the absorption and desorption process in such rubbers is proposed, and a theory is developed that considers the chemical potential gradient of the oil as the driving force. The tests are compared with experimental observations for two different oil and rubber samples, resulting in satisfactory agreement.

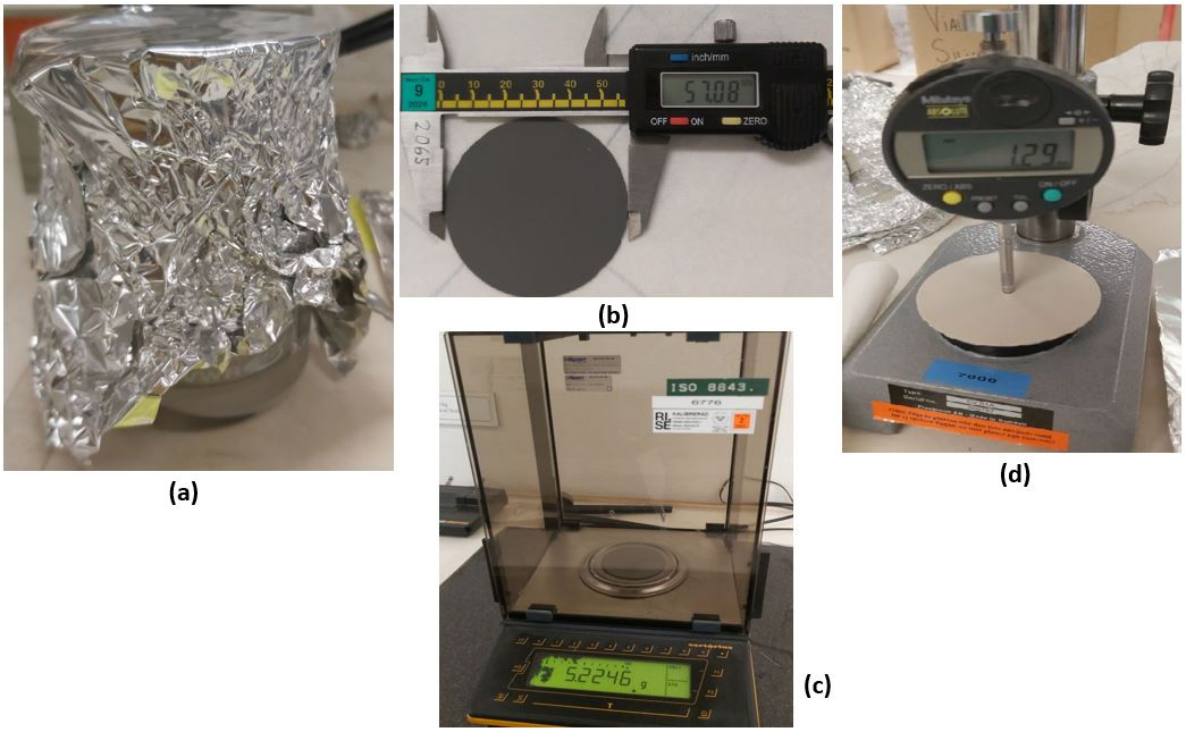


**Figure 4.14:** (a) Sample in the glass container (b) Diameter measurement (c) Weight machine (d) Thickness machine

The glass container has been filled with 200 ml of oil. Subsequently, three spherical objects have been Placed into the container and covered with the Aluminium foil to avoid the moisture that are shown in the Figure 4.14. Digital Vernier calipers measure thickness, while weight is recorded using a digital balance. Thickness is also checked with thickness measuring equipment.

# 5

# Experimental results and discussions

## 5.1 Swelling test

The test is conducted with three samples, and the mean values are calculated from these three test results.

### 5.1.1 Test with Mineral oil

The insulation and FGM rubber materials undergo a comprehensive testing and evaluation process by immersing them in mineral oil with low viscosity. This method allows us to assess how these materials interact with the oil over time.

To gather data, we measure specific parameters of the rubber samples, including their thickness, weight, and diameter. Initial observations show that, over a period of two days, there is a consistent increase in the size of the samples based on all measured parameters. This growth appears to stabilize around the third day, indicating a steady state in the absorption process.

**Table 5.1:** Swelling test on Insulation(EPDM) with Mineral oil

| Time (minutes) | Thickness (mm) | Difference (%) | Weight (gram) | Difference (%) | Diameter (mm) | Difference (%) |
|---|---|---|---|---|---|---|
| 0 | 0.97 | 0 | 2.96 | 0 | 56.78 | 0 |
| 5 | 0.99 | 2.02 | 3.05 | 2.84 | 57.05 | 0.47 |
| 30 | 1.02 | 4.34 | 3.14 | 5.90 | 57.84 | 1.86 |
| 60 | 1.04 | 6.28 | 3.23 | 8.52 | 58.56 | 3.09 |
| 180 | 1.076 | 9.74 | 3.42 | 14.15 | 59.69 | 5.00 |
| 300 | 1.10 | 12.48 | 3.58 | 18.84 | 61.01 | 7.18 |
| 1440 | 1.23 | 23.49 | 4.51 | 41.26 | 67.23 | 16.86 |
| 2880 | 1.3 | 28.40 | 4.94 | 49.90 | 69.50 | 20.15 |
| 4320 | 1.32 | 29.89 | 5.07 | 52.34 | 70.27 | 21.24 |
| 8640 | 1.32 | 30.39 | 5.14 | 53.58 | 70.39 | 21.40 |

Throughout this immersion period, it is evident that the mineral oil penetrates the rubber samples, leading to an increase in their overall dimensions. The rate of size change is correlated with the duration of exposure to the oil, highlighting the material's capacity for absorption.

The variations in size and other parameters are clearly illustrated in the accompanying figure, which provides a visual representation of the observed results and enhances our understanding of the absorption process in these rubber materials, which we can seen in the Table [5.1,5.2] and Figure [5.1,5.2].

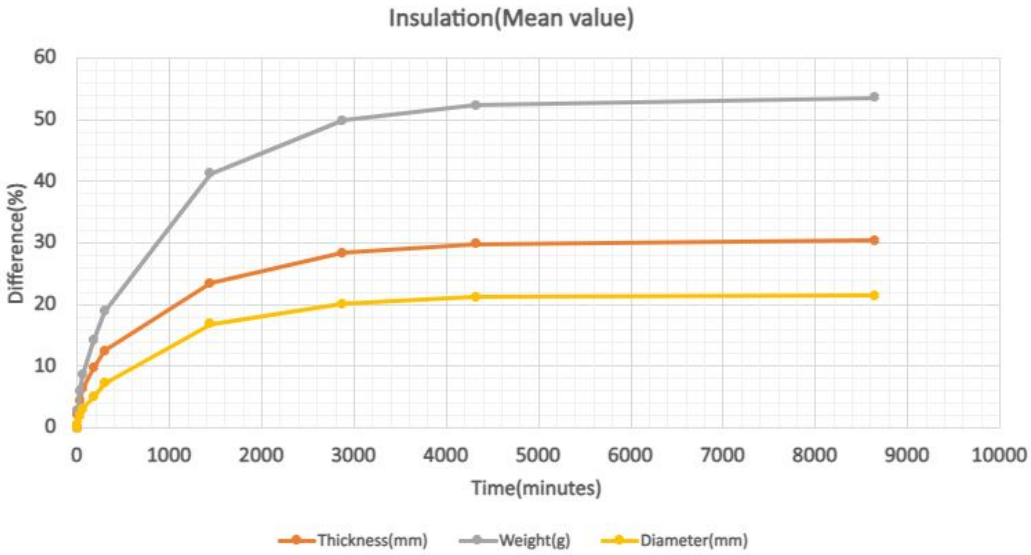


**Figure 5.1:** Swelling test on Insulation with Mineral oil(Mean value)

**Table 5.2:** Swelling test on FGM with Mineral oil

| Time (minutes) | Thickness (mm) | Difference (%) | Weight (gram) | Difference (%) | Diameter (mm) | Difference (%) |
|---|---|---|---|---|---|---|
| 0 | 1.01 | 0 | 4.20 | 0 | 56.82 | 0 |
| 5 | 1.03 | 2.27 | 4.28 | 1.81 | 57.29 | 0.82 |
| 30 | 1.06 | 4.50 | 4.36 | 3.73 | 57.72 | 1.57 |
| 60 | 1.07 | 5.75 | 4.44 | 5.33 | 57.99 | 2.04 |
| 180 | 1.10 | 8.50 | 4.59 | 8.81 | 59.15 | 4.01 |
| 300 | 1.12 | 10.29 | 4.73 | 11.77 | 60.32 | 5.98 |
| 1440 | 1.22 | 19.04 | 5.43 | 25.47 | 64.50 | 12.65 |
| 2880 | 1.27 | 22.99 | 5.66 | 29.44 | 66.64 | 15.90 |
| 4320 | 1.27 | 22.99 | 5.69 | 29.97 | 66.95 | 16.36 |
| 8640 | 1.28 | 23.25 | 5.69 | 30.06 | 66.37 | 15.49 |

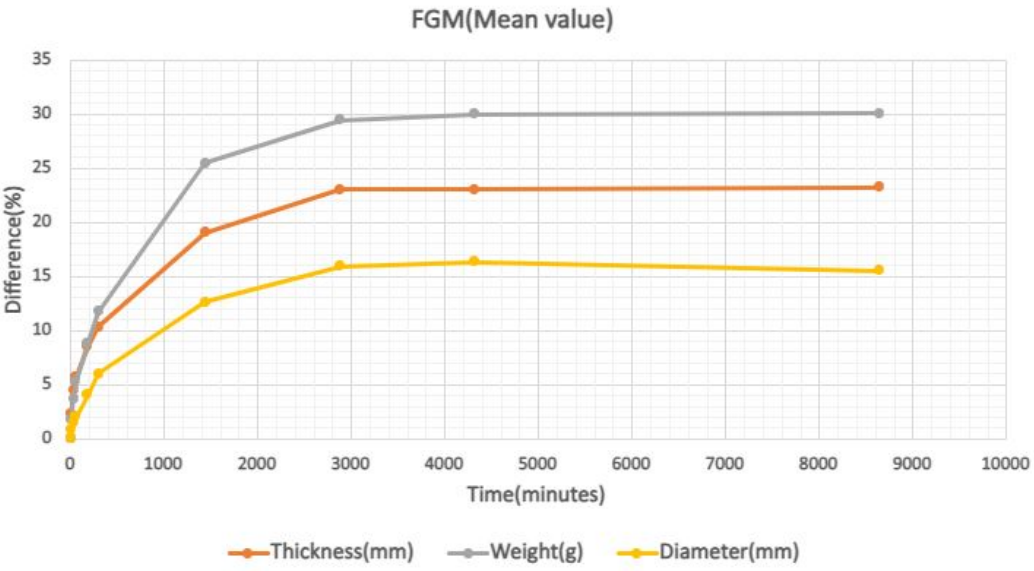


**Figure 5.2:** Swelling test on FGM with Mineral oil(Mean value)

### 5.1.2 Test with Silicone oil

The insulation and FGM rubber materials undergo thorough testing and evaluation by immersing them in silicone oil, which has a significantly higher viscosity than mineral oil. Throughout the evaluation process, we measure key parameters such as the thickness, weight, and diameter of the rubber samples to gather comprehensive data.

As we observe the samples over time, a noticeable phenomenon occurs: the size of the samples diminishes as they shrink. This reduction in size suggests that the silicone oil is effectively interacting with the materials. During this interaction, the oil begins to desorb from the rubber, and the active particles within the samples alter the color of the oil, providing a visual indication of the changes taking place.

**Table 5.3:** Swelling test on Insulation(EPDM) with Silicone oil

| Time (minutes) | Thickness (mm) | Difference (%) | Weight (gram) | Difference (%) | Diameter (mm) | Difference (%) |
|---|---|---|---|---|---|---|
| 0 | 0.96 | 0 | 2.93 | 0 | 56.55 | 0 |
| 5 | 0.96 | 0 | 2.93 | -0.29 | 56.72 | 0.29 |
| 30 | 0.96 | 0 | 2.91 | -0.90 | 56.64 | 0.15 |
| 60 | 0.96 | -0.34 | 2.89 | -1.47 | 56.57 | 0.02 |
| 180 | 0.95 | -1.04 | 2.86 | -2.47 | 56.42 | -0.24 |
| 300 | 0.95 | -1.04 | 2.84 | -3.19 | 56.26 | -0.52 |
| 1440 | 0.94 | -2.45 | 2.74 | -6.91 | 55.4 | -2.06 |
| 2880 | 0.93 | -3.16 | 2.66 | -9.84 | 54.84 | -3.08 |
| 4320 | 0.92 | -3.88 | 2.60 | -11.98 | 54.43 | -3.82 |
| 8640 | 0.91 | -5.32 | 2.50 | -15.81 | 53.46 | -5.62 |

The relationship between time and the observed size reduction is particularly striking, as the effects become more pronounced the longer the samples remain immersed in the oil. The resulting differences and changes in the samples are clearly illustrated in the accompanying Table [5.3,5.4] and Figure [5.3,5.4] highlighting the significant impact of the silicone oil on the rubber materials.

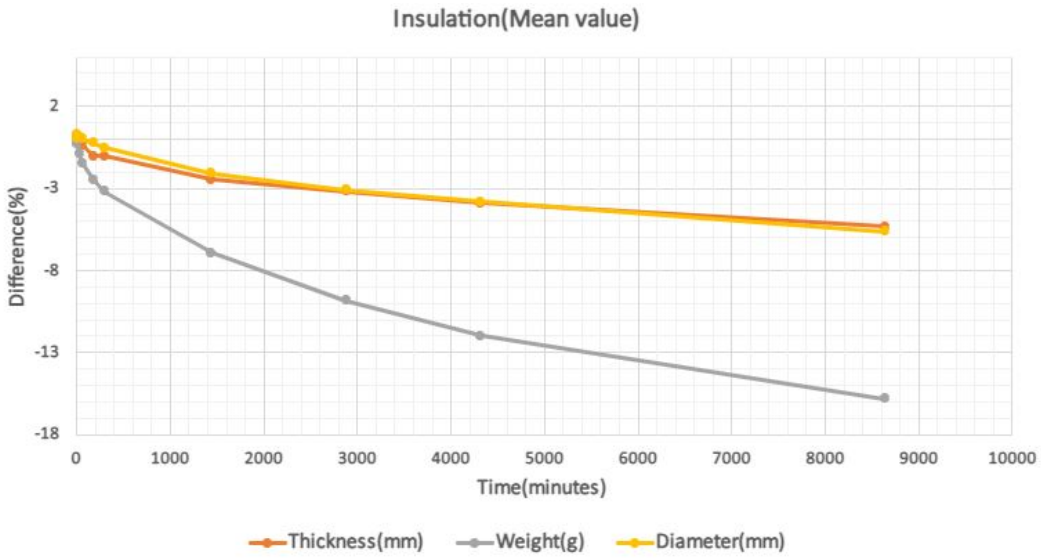


**Figure 5.3:** Swelling test on Insulation(EPDM) with Silicone oil(Mean value)

**Table 5.4:** Swelling test on FGM with Silicone oil

| Time (minutes) | Thickness (mm) | Difference (%) | Weight (gram) | Difference (%) | Diameter (mm) | Difference (%) |
|---|---|---|---|---|---|---|
| 0 | 1.01 | 0 | 4.21 | 0 | 56.75 | 0 |
| 5 | 1.01 | 0 | 4.21 | -0.1 | 56.71 | -0.08 |
| 30 | 1.01 | 0 | 4.19 | -0.32 | 56.55 | -0.36 |
| 60 | 1.01 | 0 | 4.19 | -0.59 | 56.41 | -0.61 |
| 180 | 1.01 | 0 | 4.17 | -0.98 | 56.33 | -0.75 |
| 300 | 1.00 | -0.98 | 4.16 | -1.36 | 56.19 | -0.99 |
| 1440 | 1.00 | -1.32 | 4.09 | -3.05 | 55.85 | -1.61 |
| 2880 | 1.00 | -1.32 | 4.03 | -4.40 | 55.33 | -2.54 |
| 4320 | 0.99 | -2.32 | 3.99 | -5.51 | 55.11 | -2.94 |
| 8640 | 0.99 | -2.65 | 3.90 | -7.68 | 54.39 | -4.25 |

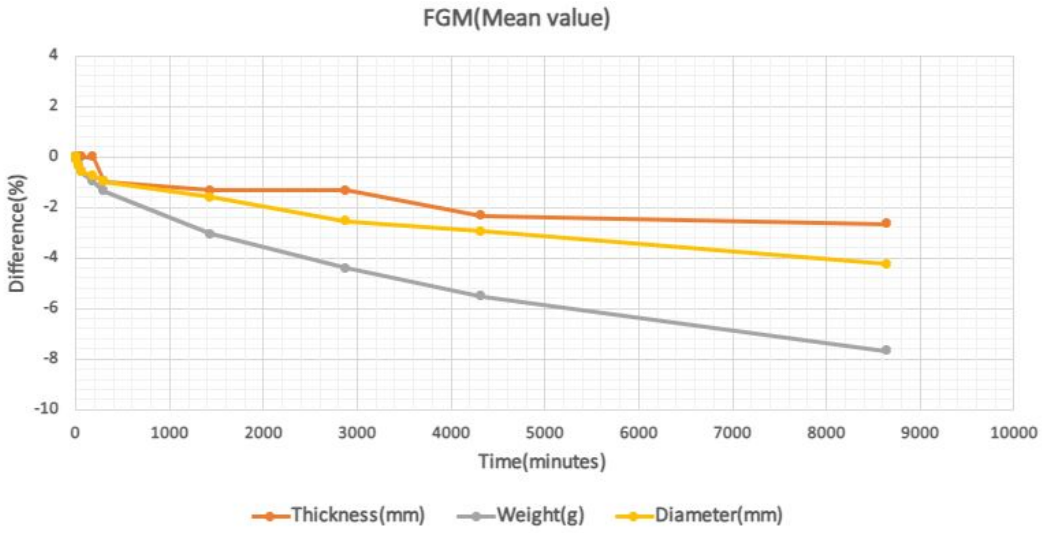


**Figure 5.4:** Swelling test on FGM with Silicone oil(Mean value)

## 5.2 Breakdown tests

### 5.2.1 AC Breakdown test

The results of the dielectric breakdown performance of the FGM indicate that breakdown occurs at the center of the sample. This is due to the increasing external electric field as voltage is applied, which leads to a rise in current. This type of breakdown is classified as conductive breakdown, also known as intrinsic breakdown[2.1.1]. The breakdown point can be observed in the accompanying Figure 5.5(a)(b)(c).

The dielectric breakdown in the insulation sample occurs at a triple point, due to the electric field is scattered towards the triple points and breakdown traces for insulation, rather than for the FGM, which we discussed previously in section 2.1.3. The breakdown point for this test is also illustrated in the Figure 5.5(d)(e)(f).

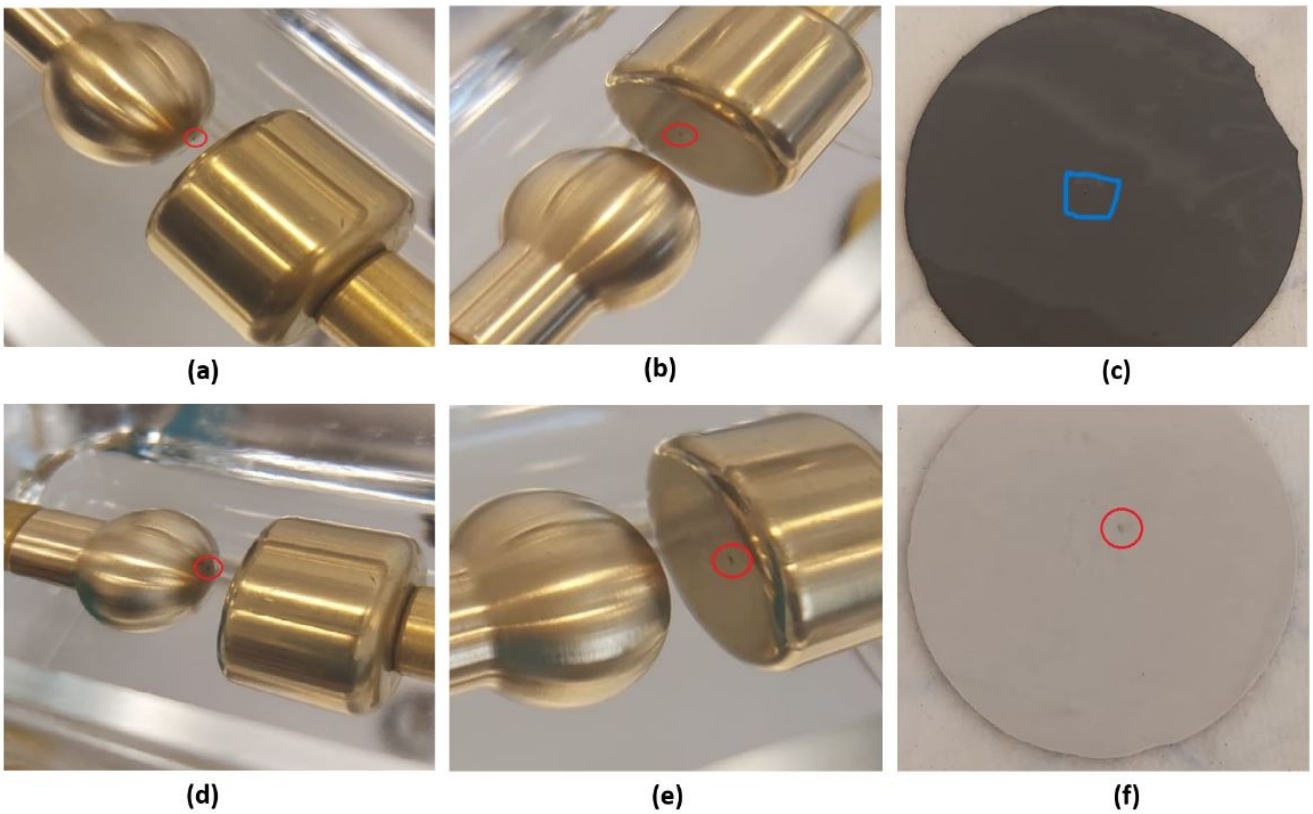


**Figure 5.5:** ACBD Testing (a) BD point on the HV electrode on FGM ;(b) BD point on the Ground electrode on FGM ;(c) BD point on the FGM sample;(d) BD point on the HV electrode on Insulation ;(e) BD point on the Ground electrode on Insulation ;(f) BD point on the Insulation sample

The simulation results provide a comprehensive analysis of the electric field distribution when different types of insulating oils, each with varying permittivity, are employed as surrounding mediums. As illustrated in the Figure 5.6, The applied voltage for insulation is 50 kV, while for the FGM it is 10 kV. A frequency domain study with 50 Hz is used in the simulation.

Together, these observations highlight the significant impact of the choice of insulating oil on electric field behavior in the studied configuration.

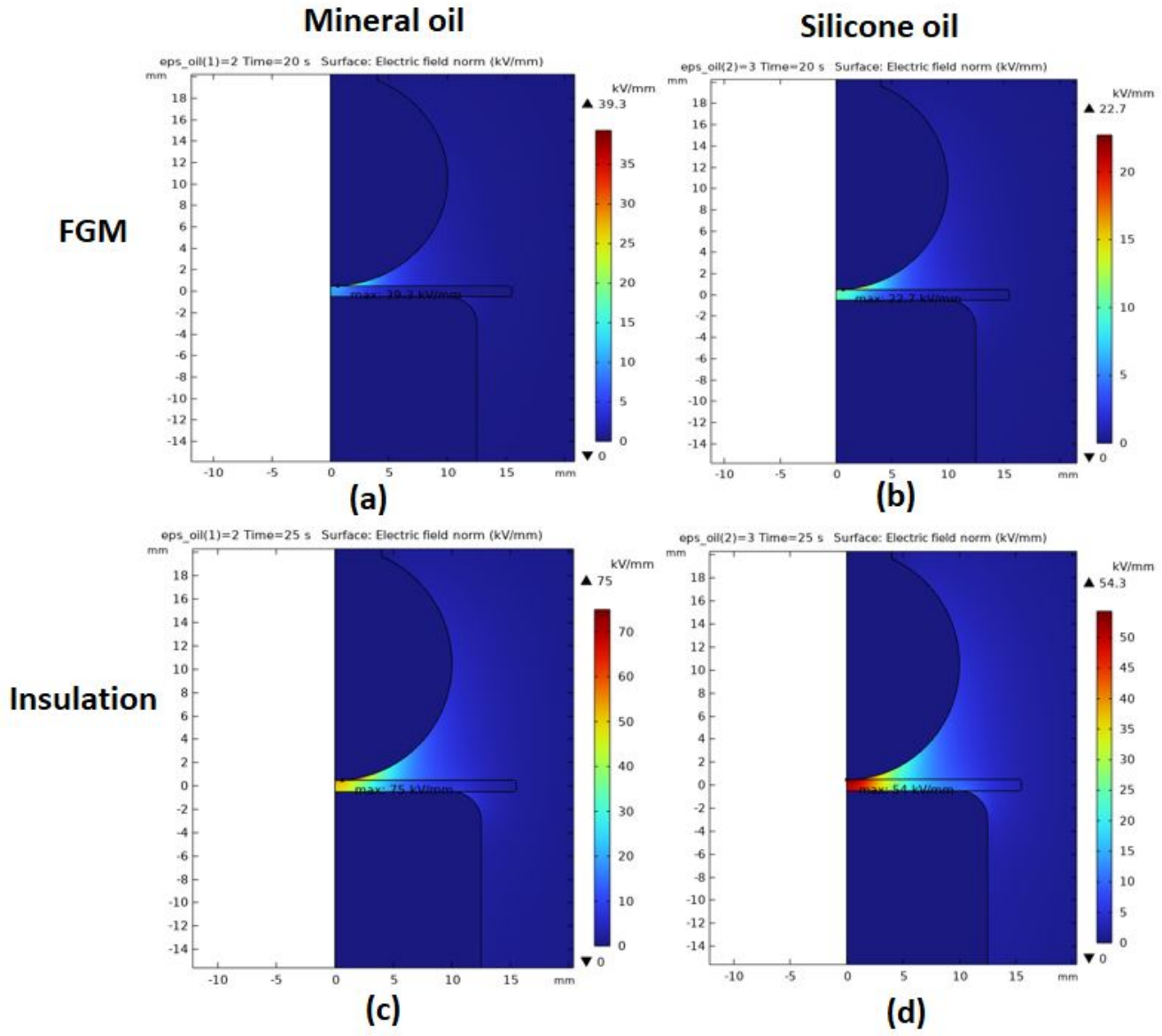


**Figure 5.6:** ACBD testing:(a) Field distribution on FGM with mineral oil ;(b) Field distribution on FGM with Silicone oil;(c) Field distribution on Insulation with mineral oil; (d) Field distribution on Insulation with Silicone oil

The FGM and insulation sample was tested with mineral oil and silicone oil. Through our simulations, we observed that the electric field was higher near the triple point when using mineral oil. This is attributed to the lower permittivity of mineral oil, which causes the electric field to concentrate in the oil. Consequently, we anticipated a lower breakdown strength for the mineral oil used in the FGM and insulation sample, which is illustrated in the Figure 5.6 (a) and (c).

The permittivity of silicone oil is higher, which causes the more electric field pushes to the sample, as illustrated in the figure 5.6 (b) and (d). This results in a higher breakdown strength for silicone oil when used with the FGM and insulation sample.

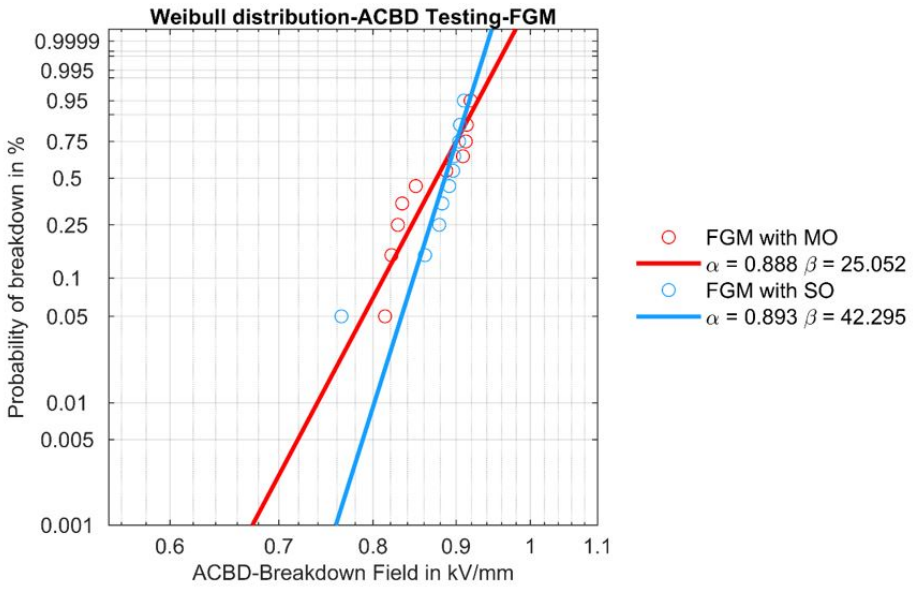


**Figure 5.7:** Weibull plots(normalized value) for AC breakdown testing on FGM with MO and SO

The Weibull distribution plot(normalized value) shows that silicone oil has a higher breakdown strength than mineral oil, as illustrated in the Figure 5.7 and 5.8. This indicates that silicone oil is positioned to the right of mineral oil on the plot, demonstrating its superior breakdown strength compared to mineral oil. Some results from the mineral oil tests exhibited slight deviations, likely due to the aging of the oil. Nonetheless, breakdown still occurred at the triple point, as depicted in Figure 5.8.

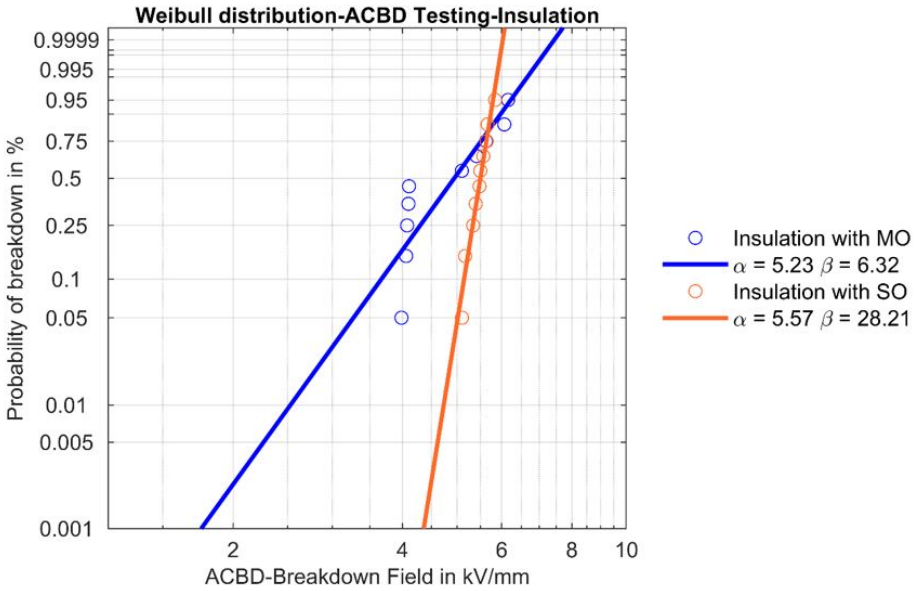


**Figure 5.8:** Weibull plots(normalized value) for AC breakdown testing on Insulation(EPDM) with MO and SO

### 5.2.2 DC Breakdown test

The DCBD testing was performed using a newly designed test cell specifically engineered for this purpose[19]. In this testing setup, the distribution of the electric field is significantly affected by the conductivity properties of the materials being evaluated.The applied ramping DC voltage is

not truly a pure direct current (DC). The breakdown strength is influenced by the permittivity, as we explained before in the AC breakdown test[5.2.1].

The voltage rate selected for the FGM is 500V/s, while the insulation is 2kV/s. This will typically cause breakdown to occur between 10s and 20s, in accordance with IEC 60243-2[19].

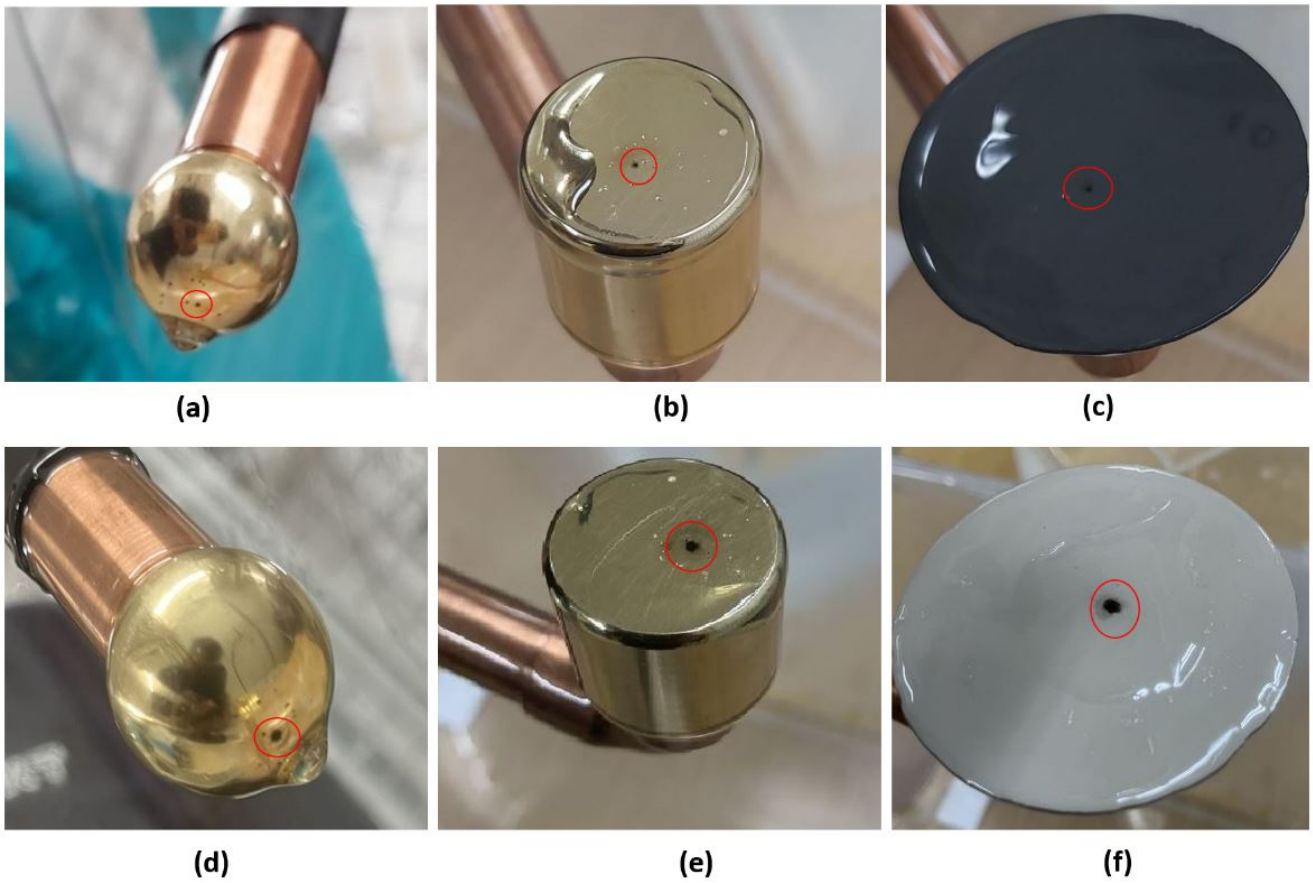


**Figure 5.9:** DCBD Testing (a) BD point on the HV electrode on FGM ;(b) BD point on the Ground electrode on FGM ;(c) BD point on the FGM sample;(d) BD point on the HV electrode on Insulation ;(e) BD point on the Ground electrode on Insulation ;(f) BD point on the Insulation sample

The breakdown paths for insulation are more scattered, which relates to dielectric breakdown. In contrast, the electric field is more concentrated in the center for FGM due to conduction breakdown. The concentration of these electric fields depends on the permittivity of the insulating liquid,which we can observed in the Figure 5.9.

The Weibull distribution has been observed for the FGM sample, indicating that the breakdown strength occurs at the center of the electrode[2.1.1]. This is due to the high electric field concentration near the center, resulting in conductive breakdown, as shown in Figure 5.10.

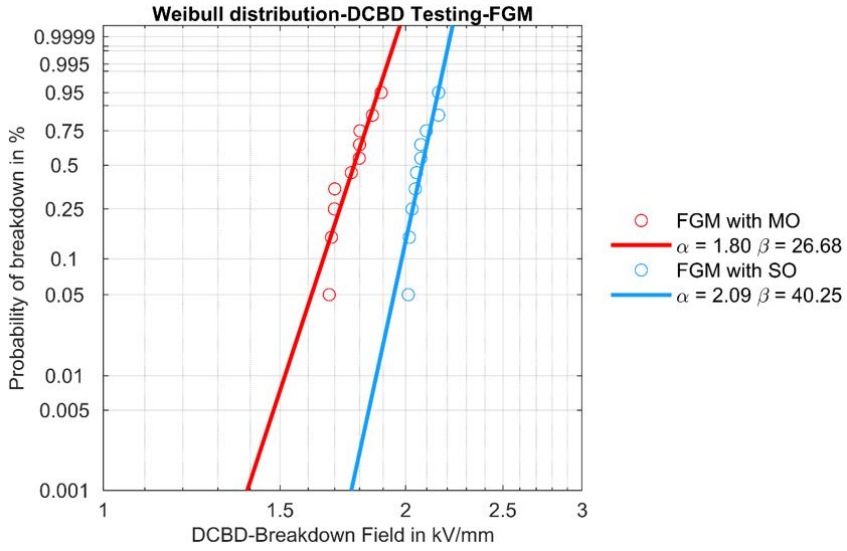


**Figure 5.10:** Weibull plots(normalized value) for DC breakdown testing on FGM with MO and SO

Conversely, the distribution plots(normalized value) for insulation sample reveal that breakdown occurs at the sample due to the triple point, which can be seen in Figure 5.11.

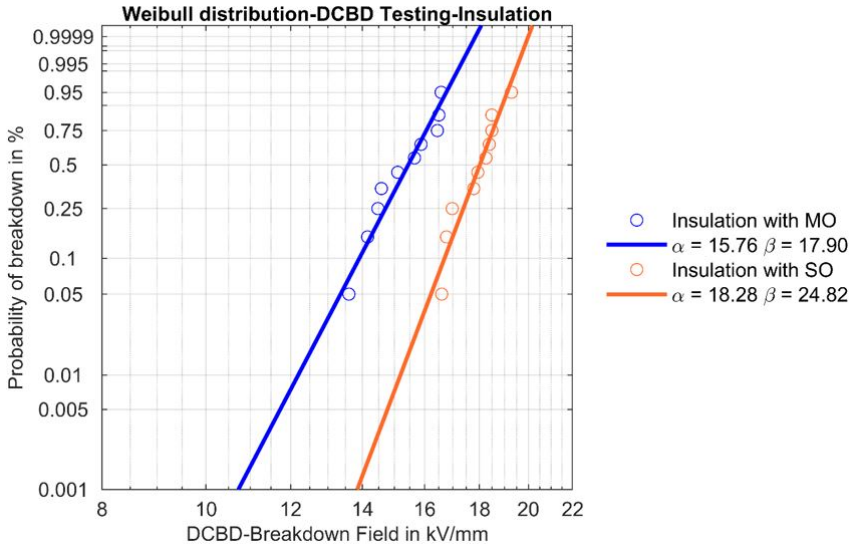


**Figure 5.11:** Weibull plots(normalized value) for DC breakdown testing on Insulation(EPDM)) with MO and SO

#### 5.2.2.1 Moulded sample(short time test)

The DCBD testing was carried out on the newly developed molded electrode made from FGM. The voltage was applied at a rate of 0.5 kV per second during the testing process[19]. Observations revealed that the breakdown point in the sample occurs at a location where the electric field is highly concentrated, specifically at the center of the electrode. This phenomenon was visually represented in the accompanying figure 5.12, which illustrates the electric field distribution throughout the electrode. The applied voltage for the test is 25 kV used in the simulation.

Furthermore, the simulation results highlighted a significant enhancement of the electric field in the central region of the electrode, indicating that this area is particularly susceptible to

breakdown under the applied voltage conditions. The detailed visual representation corroborates these findings and serves to emphasize the critical role of the electrode's geometry in electric field distribution.

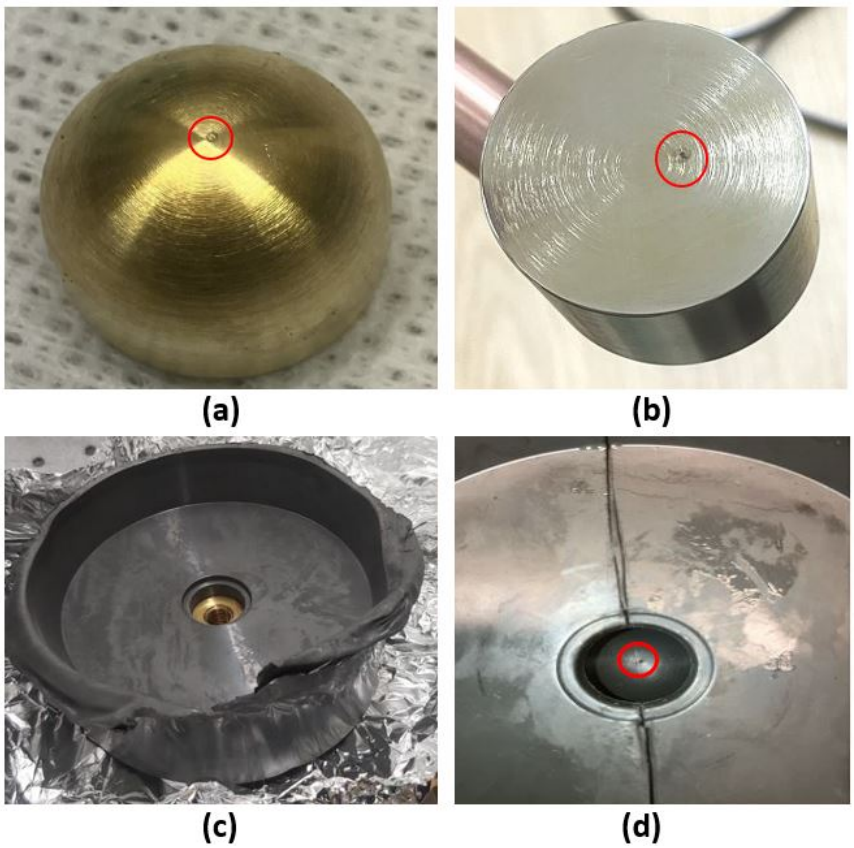


**Figure 5.12:** (a) HV electrode BD point (b) Ground electrode BD point (c) Moulded electrode sample (d) BD point on the moulded electrode sample

#### 5.2.2.2 Comparison of DCBD testing with moulded Electrode sample

The comparison of DCBD testing with the molded sample, evaluated across three separate tests, indicates that the occurrence of breakdown is uniform in all samples. This pattern is comparable to the results obtained from ACBD testing conducted on samples that incorporate an insulating medium(oil).

The Weibull distribution plot indicates that the lower breakdown strength of mineral oil is attributed to its lower permittivity, while the higher breakdown strength of silicone oil results from its higher permittivity. Additionally, the breakdown strength of the molded electrode sample is greater than the tests with Mineral oil and Silicone oil, as the molding process eliminates the triple point, and the electric field concentrated in the center of the sample, as depicted in the Figure 5.13.

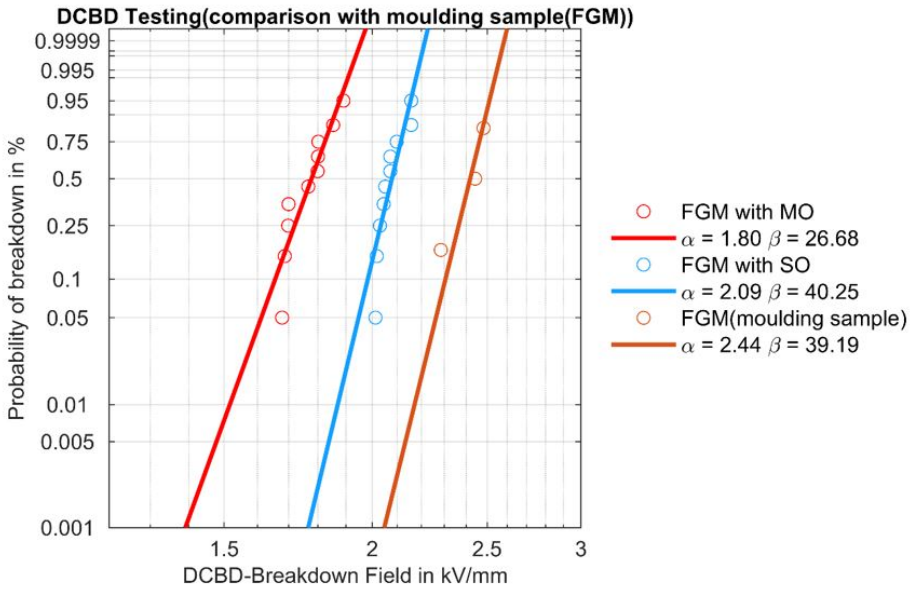


**Figure 5.13:** Weibull plots(normalized value) for DC breakdown testing on FGM(comparison with Moulded sample)

### 5.2.3 Lightning Impulse Breakdown test

The LIBD testing was conducted on insulation material.The minimum voltage applied using the impulse generator is 30 kV. If the breakdown occurs below this level, the waveform cannot be tracked in data acquisition. Therefore, LIBD testing was not performed on the FGM. The tests were performed using both mineral oil and silicone oil as surrounding medium. When using mineral oil, the electric field is directed away from the sample due to the lower permittivity, while the electric field pushes into the sample by using silicone oil due to the higher permittivity, which we explained before in the AC breakdown test[5.2.1]. The breakdown point on the surface of the electrode is also depicted in the Figure 5.14.

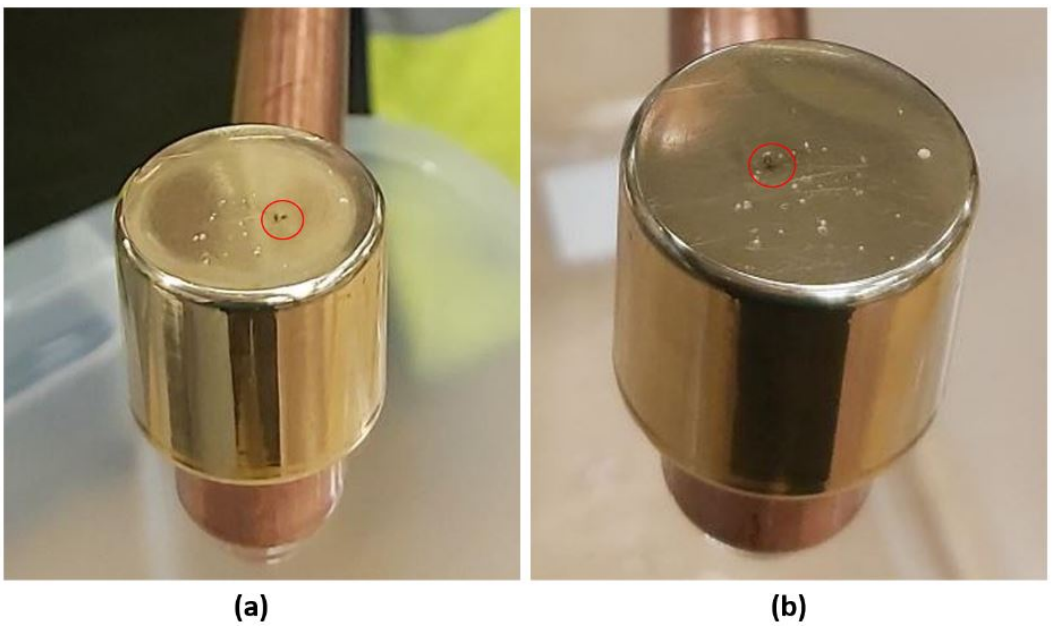


**Figure 5.14:** LIBD testing (a) BD point on the surface of the ground electrode on test 1 (b) BD point on the surface of the ground electrode on test 2

A simulation illustrating the distribution of the electric field can be seen in the Figure 5.15. The

voltage applied for the simulation in the test is 100 kV with the time of 2$\mu$s which is the time that the voltage reaches to the maximum in LI waveform.

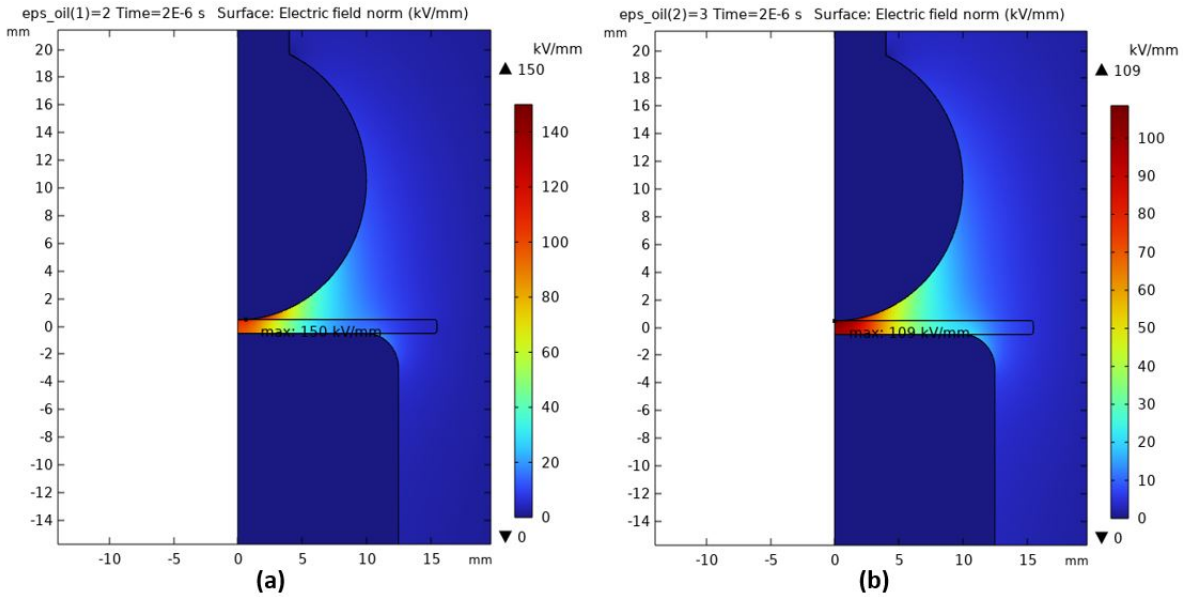


**Figure 5.15:** Simulation for the LIBD Testing(a) Electric field distribution with mineral oil (b) Electric field distribution with Silicone oil

The distribution plots illustrating the breakdown probability for LIBD testing on Insulation sample with Mineral oil and silicone oil used as surrounding medium are presented in the figure 5.16 below. The weibull distribution plots shows that the higher breakdown strength for the Silione oil, due to the higher permittivity and lower breakdown streanth for the mineral oil, due to the lower permittivity.

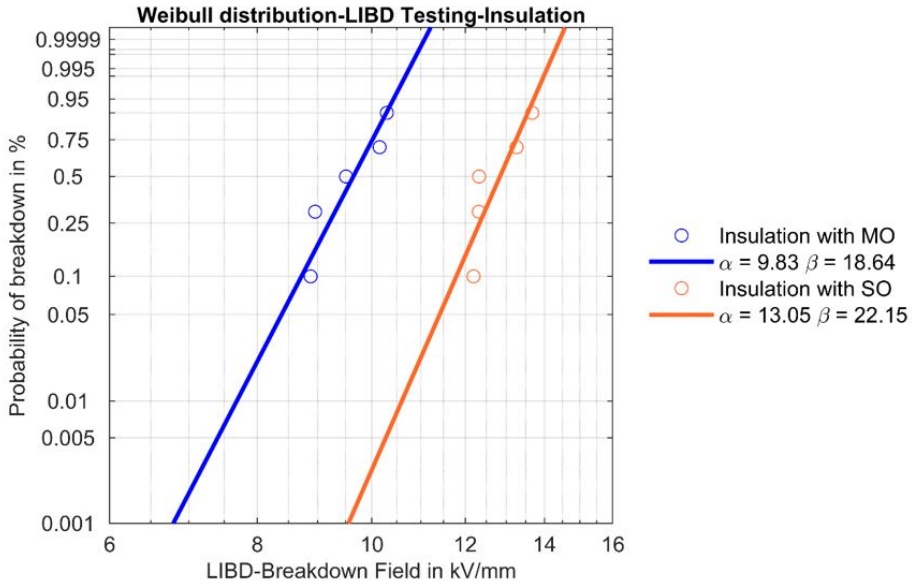


**Figure 5.16:** Weibull plots(normalized value) for LI breakdown testing on Insulation(EPDM) with MO and SO

# 6
# Conclusion

A test setup for the test cell was developed from scratch during this project. This process involved several steps, including FEM simulation, CAD design, procurement of all components, assembly of the test connections, and integration for operation, including the control unit (control the DC source during the test) followed by data collection and evaluation. The test cell was designed for an applied voltage of 150 kV, and the electrode was created in accordance with IEC 60243-2 standards[19] for DC breakdown testing and IEC 60243-3 standards[20] for LI breakdown testing.

Breakdown testing and electric field analysis were studied from a technical perspective and applied to design and testing processes. The swelling tests for the rubber samples were conducted using mineral oil and silicone oil to investigate the absorption and desorption properties of the material in these oils. This testing aimed to design a new type of sample that could be tested without the surrounding medium, thereby eliminating the triple point.

The two different oils with varying permittivity and viscosity were used for testing to trace the electric field stress and observe breakdown in the sample.The insulating oil was tested for breakdown voltage, relative permittivity, dielectric dissipation factor, DC resistivity, and water content. ACBD testing has been conducted on various materials, along with dielectric testing of rubber materials for HVDC applications in the material lab. With the existing setup, ACBD testing was conducted on the insulation and FGM in accordance with IEC 60243-1 standards[18].

During the DC breakdown testing(short time test), a high voltage of 150 kV was applied to the test cell is achieved. Each test yielded observable marks on the surface of the electrodes, which are illustrated in the accompanying Figure 5.9 [a,b,d,e]. It is crucial to note that the electrode sets must be replaced after every ten tests to maintain accuracy and reliability in the results. Furthermore, it is necessary to polish the electrodes after each use to ensure a smooth surface, preventing any surface irregularities that could affect testing outcomes.

The high voltage electrode was moulded using a FGM to eliminate triple points and the DCBD test(short time test) was conducted. Additionally, the surface of the ground electrode is significantly longer than standard specifications, and the sharp edges are designed to reduce the high electric field intensity near the electrode's edges. Looking ahead, we are committed to enhancing the test cell design. Moreover, we will investigate the feasibility of moulding both the HV electrode and the ground electrode, which could streamline the testing process and improve overall results for perform the endurance test in the future.

# Bibliography


[1] E. Kuffel, W.S. Zaengl and J. Kuffel, "High Voltage Engineering Fundamental", 2nd edition, ISBN 0 7506 3634 3, Butterworth-Heinemann, Oxford, 2000.

[2] C.L. Wadhwa, "High Voltage Engineering", Second Edition, New Age International (P) Ltd., Publishers, New Delhi, 2007.

[3] K.C. Kao. Trans. AIEEE Elec. Ins. Vol. E1-11 (1976), pp. 121–128.

[4] R.H. Fowler and L.W. Nordheim. Proc. Roy. Soc. London 119 (1928), p. 173; 124 (1929),p. 699.

[5] J.K. Nelson. Dielectric Fluids in Motion. IEEE Electrical Insulation Magazine, Vol. 10,No. 11 994, pp. 16–28.

[6] J.C. Lacroix, P.A. Hen and E.J. Hopfinger. J. Fluid Mech. 69 (1975), p. 539.

[7] N.J. Felici. Direct Current 2 (1971), p. 147.

[8] N.J. Felici and J.C. Lacroix. J. Electrost. 5 (1978), p. 135.

[9] J.D. Cross, M. Nakans and S. Savanis. J. Electrost. 7 (1979), p. 361.

[10] B.D. Popovic. Introductory Engineering Electromagnetics. Addison-Wesley, 1971.

[11] D. Vitkovitch. Field Analysis: Experimental and Computational Methods. D. Van Nostrand,1966.

[12] P. Moon and D.E. Spencer. Field Theory for Engineers. D. Van Nostrand, 1961; Field Theory Handbook. Springer, 1961.

[13] J.D. Kraus and K.R. Carver. Electromagnetics (2nd edn). McGraw-Hill, New York, 1973.

[14] IEC 60052, "Voltage measurement by means of standard air gaps", Third edition, International Electrotechnical Commission (IEC), Geneva, 2002.

[15] F.F. Dall'Agnol and V.P. Mammana, "Solution for the electric potential distribution produced by sphere-plane electrodes using the method of images", Revista Brasileira de Ensino de Fisica, Vol. 31, No. 3, Article No. 3503, September 2009.

[16] M.A. Shallal and J.A. Harrison, "Electric, field potential and capacitance of a sphere-plane electrode system", Proceedings of The Institution of Electrical Engineers, Vol.116, No. 6, pp. 1115-1118, June 1969.

[17] IEC 60247:2004,Insulating liquids - Measurement of relative permittivity, dielectric dissipation factor (tan d) and d.c. resistivity

[18] IEC 60243-1:2013, Electric strength of insulating materials – Test methods – Part 1: Tests at power frequencies

[19] IEC 60243-2:2013, Electric strength of insulating materials -Test methods - Part 2: Additional requirements for tests using direct voltage

[20] IEC 60243-3:2014, Electric strength of insulating materials –Test methods – Part 3: Additional requirements for 1,2/50 µs impulse tests

[21] IEC 60156:2018,Insulating liquids - Determination of the breakdown voltage at power frequency - Test method

[22] ASTM D6304-20,Standard Test Method for Determination of Water in Petroleum Products, Lubricating Oils, and Additives by Coulometric Karl Fischer Titration

[23] Treloar, L. R. G.The Physics of Rubber Elasticity', Clarendon Press, Oxford, 1958

[24] Fabiani, Davide and Simoni, Luciano, fabiani 2005 discussion,Discussion on application of the Weibull distribution to electrical breakdown of insulating materials,IEEE transactions on dielectrics and electrical insulation, volume 12,number 1, pages 11–16, year 2005,publisher IEEE.

[25] High Voltage Engineering Laboratory-Lightning Impulse Testing.

[26] G. Mazzanti, M. Marzinotto, "Advanced electro-thermal life and reliability model for high voltage cable systems including accessories",IEEE Electr. Insul. Mag., vol. 33, no. 3, 2017, pp. 17–25

[27] A. Plesa, D. Mihai, P.V.Notingher, "Polymeric Compound for Electric Field Control of Power Cable Accessories", 4th International Symposium on Advanced Topics in Electrical Engineering (ATEE2004), November 25-26, Bucharest, Section 5, Paper 11, Vol. II, 2004, pp. 277–283, ISBN 973-7728-31-9.

[28] L. Donzel, T. Christen, R. Kessler, F. Greuter, H. Gramespacher, "Silicone composites for HV applications based on microvaristors", in Proceedings of the 2004 IEEE International Conference on Solid Dielectrics (ICSD 2004), 2004, pp. 403–406.

[29] P. N. Nelson, "High dielectric constant materials for primary voltage cable terminations", IEEE Transaction on Power Apparatus and Systems, Vol. PAS-103, No. 11, 1984, pp. 3211–3216.

[30] J. P. Rivenc, T. Lebey, "An Overview of Electrical Properties for Stress Grading Optimization", IEEE Transactions on Dielectrics and Electrical Insulation, Vol. 6, No. 3, 1999, pp. 309–318.

[31] T. Christen, L. Donzel and F. Greuter, "Nonlinear resistive electric field grading part 1: Theory and simulation", IEEE Electr. Insul. Mag.,vol. 26, no. 6, 2010, pp. 48–60.

[32] L. Donzel, F. Greuter, T. Christen, "Nonlinear Resistive Electric Field Grading Part 2: Materials and Applications", IEEE Electrical Insulation Magazine, Vol. 27, No. 2, 2010, pp. 18–29.

[33] G. Mazzanti, M. Marzinotto, "Advanced electro-thermal life and reliability model for high voltage cable systems including accessories", IEEE Electr. Insul. Mag.,vol. 33, no. 3, 2017, pp. 17–25.

[34] Influence of FGM layer on the distribution of the electric field in DC cable joints insulations Lucian Viorel Taranu, Petru V. Notingher, Member IEEE, Cristina Stancu, Member IEEE.

[35] Springer Handbook of Engineering Statistics 1. Engineering - Statistical methods I. Pham, Hoang 620'.0072 ISBN-13: 9781852338060 ISBN-10: 1852338067; chapter 3. weibull distributions and their applications .

[36] Direct Current Electrical Performances of Cable Accessory Insulation EPDM Modified by Grafting Polar-Group Compound Zhong-Yuan Li, Wei-Feng Sun ,Jian Zhang, Jian-Quan Liang , Lei Wang and Ke-Xin Zhang.

[37] Mazzanti, G. Life and reliability models for high voltage DC extruded cables. IEEE Electr. Insul. Mag. 2017, 33, 42–52.

[38] Hanley, T.L.; Burford, R.P.; Fleming, R.J.; Barber, K.W. A general review of polymeric insulation for use in HVDC cables. IEEE Electr. Insul. Mag. 2003, 19, 13–24.

[39] Lewis, T.J. Nanometric Dielectrics. IEEE Trans. Dielectr. Electr. Insul. 1994, 1, 812–825.

[40] Tanaka, T.; Montanari, G.C.; Mulhaupt, R. Polymer nanocomposites as dielectrics and electrical insulation-perspectives for processing technologies, material characterization and future applications. IEEE Trans. Dielectr. Electr. Insul. 2004, 11, 763–784.

[41] Venkatesulu, B.; Thomas, M.J. Corona aging studies on silicone rubber nanocomposites. IEEE Trans. Dielectr. Electr. Insul. 2010, 17, 625–634.

[42] Tu, Y.P.; Zhou, F.W.; Cheng, Y.; Jiang, H.; Wang, C.; Bai, F.J.; Lin, J. The control mechanism of micron and nano SiO2/epoxy composite coating on surface charge in epoxy resin. IEEE Trans. Dielectr. Electr. Insul. 2018, 25, 1275–1284

[43] Li, Z.Y.; Sun, W.F.; Zhao, H. Significantly improved electrical properties of photo-initiated auxiliary crosslinking EPDM used for cable termination. Polymers 2019, 11, 2083.
[44] Wang, X.; Nelson, J.K.; Schadler, L.S.; Hillborg, H. Mechanisms leading to nonlinear electrical response of a nano p-SiC/silicone rubber composite. IEEE Trans. Dielectr. Electr. Insul. 2010, 17, 1687–1696.
[45] Li, Z.; Yang, Z.; Xing, Y.; Zhu, W.; Su, J.; Kong, X.; Jiang, J.; Du, B. Improving the electric field distribution in stress cone of HTS DC cable terminals by nonlinear conductive epoxy/ZnO composites. IEEE Trans. Appl. Supercond. 2019, 29, 7000305.
[46] Li, J.; Du, B.; Kong, X.X.; Li, Z.L. Nonlinear conductivity and interface charge behaviors between LDPE and EPDM/SiC composite for HVDC cable accessory. IEEE Trans. Dielectr. Electr. Insul. 2017, 24, 1566–1573.
[47] Xue, J.Y.; Chen, J.H.; Dong, J.H.; Wang, H.; Li, W.D.; Deng, J.B.; Zhang, G.J. The regulation mechanism of SiC/epoxy coatings on surface charge behavior and flashover performance of epoxy/alumina spacers. J. Phys. D Appl. Phys. 2019, 52, 405502.
[48] Han, Y.; Li, S.; Min, D. Nonlinear conduction and surface potential decay of epoxy/SiC nanocomposites. IEEE Trans. Dielectr. Electr. Insul. 2017, 24, 3154–3164.
[49] Li, Z.; Su, J.; Du, B.; Hou, Z.; Han, C. Inhibition effect of graphene on space charge injection and accumulation in low-density polyethylene. Nanomaterials 2018, 8, 956.
[50] Zhou, Y.; Hu, J.; Dang, B.; He, J.L. Mechanism of highly improved electrical properties in polypropylene by chemical modification of grafting maleic anhydride. J. Phys. D Appl. Phys. 2016, 49, 415301.
[51] Dielectric strength behaviour and mechanical properties of transperant insulation materials suitable to optical monitoring of partial discharges;Chaiyaporn Lothongkam;2014.
[52] ASTM D3616-95(2019):Standard Test Method for Rubber—Determination of Gel, Swelling Index, and Dilute Solution Viscosity
[53] Swelling Behavior of Elastomers under Water, Oil, and Acid Written By Sayyad Zahid Qamar, Maaz Akhtar and Tasneem Pervez Submitted: 23 October 2020 Reviewed: 26 October 2020 Published: 27 October 2021
[54] Chauvet, C., Laurent, C. (1993). Weibull statistics in short-term dielectric breakdown of thin polyethylene films. Laboratoire de Génie Électrique, CNRS, Université Paul Sabatier, Toulouse, France.
[55] The Vanderbilt-RUBBER HANDBOOK; Fourteenth Edition; page 138-198.
[56] Roger S. Amos, Geoffrey William Arnold Dummer (1999). Newnes Dictionary of Electronic (4th ed.). Newnes. p. 83. ISBN 0-7506-4331-5.

**DEPARTMENT OF SOME SUBJECT OR TECHNOLOGY**
**CHALMERS UNIVERSITY OF TECHNOLOGY**
Gothenburg, Sweden
www.chalmers.se


CHALMERS
UNIVERSITY OF TECHNOLOGY